Title
Network anatomy in logopenic variant of primary progressive aphasia

Journal
Human Brain Mapping, 44(11)

ISSN
1065-9471

Authors
Mandelli, Maria Luisa
Lorca-Puls, Diego L
Lukic, Sladjana
et al.

Publication Date
2023-08-01

DOI
10.1002/hbm.26388

Peer reviewed

Received: 22 December 2022 | Revised: 21 April 2023 | Accepted: 17 May 2023

DOI: 10.1002/hbm.26388

RESEARCH ARTICLE

WILEY

Network anatomy in logopenic variant of primary progressive aphasia

Maria Luisa Mandelli[1] | Diego L. Lorca-Puls[1,2] | Sladjana Lukic[1,3] | Maxime Montembeault[1,4] | Andrea Gajardo-Vidal[1,5] | Abigail Licata[1] | Aaron Scheffler[6] | Giovanni Battistella[1,7] | Stephanie M. Grasso[8] | Rian Bogley[1] | Buddhika M. Ratnasiri[1] | Renaud La Joie[1] | Nidhi S. Mundada[1] | Eduardo Europa[9] | Gil Rabinovici[1] | Bruce L. Miller[1] | Jessica De Leon[1] | Maya L. Henry[8] | Zachary Miller[1] | Maria Luisa Gorno-Tempini[1]

[1]Memory and Aging Center, Department of Neurology, University of California, San Francisco, California, USA

[2]Sección de Neurología, Departamento de Especialidades, Facultad de Medicina, Universidad de Concepción, Concepción, Chile

[3]Department of Communication Sciences and Disorders, Adelphi University, Garden City, New York, USA

[4]Department of Psychiatry, Douglas Mental Health University Institute, McGill University, Montréal, Canada

[5]Faculty of Health Sciences, Universidad del Desarrollo, Concepción, Chile

[6]Department of Epidemiology and Biostatistics, University of California, San Francisco, California, USA

[7]Department of Otolaryngology, Head and Neck Surgery, Massachusetts Eye and Ear and Harvard Medical School, Boston, Massachusetts, USA

[8]Department of Speech, Language, and Hearing Sciences, University of Texas, Austin, Texas, USA

[9]Department of Communicative Disorders and Sciences, San Jose State University, San Jose, California, USA

Correspondence
Maria Luisa Mandelli, Department of Neurology, UCSF, 675 Nelson Rising Lane, Mission Bay Campus, San Francisco, CA 94158, USA.
Email: marialuisa.mandelli@ucsf.edu

Funding information
Alzheimer's Disease Research Centre of California, Grant/Award Number: 03-75271 DHS/ADP/ARCC; Foundation for the National Institutes of Health, Grant/Award Numbers: K24DC015544, NIA K99AG065501, NIA P01 AG019724, NIA P30 AG062422, NIA P50 AG03006, NIDCD R01DC016291, NINDS R01 NS050915; Larry L. Hillblom Foundation; John Douglas French Alzheimer's Foundation; Koret Family Foundation; Consortium for Frontotemporal Dementia Research; McBean Family Foundation; Career Scientist Award; Chilean National Agency for Research and Development, Grant/Award Numbers: ANID BECAS-CHILE 74200065, ANID BECAS-CHILE 74200073

Abstract

The logopenic variant of primary progressive aphasia (lvPPA) is a neurodegenerative syndrome characterized linguistically by gradual loss of repetition and naming skills resulting from left posterior temporal and inferior parietal atrophy. Here, we sought to identify which specific cortical loci are initially targeted by the disease (epicenters) and investigate whether atrophy spreads through predetermined networks. First, we used cross-sectional structural MRI data from individuals with lvPPA to define putative disease epicenters using a surface-based approach paired with an anatomically fine-grained parcellation of the cortical surface (i.e., HCP-MMP1.0 atlas). Second, we combined cross-sectional functional MRI data from healthy controls and longitudinal structural MRI data from individuals with lvPPA to derive the epicenter-seeded resting-state networks most relevant to lvPPA symptomatology and ascertain whether functional connectivity in these networks predicts longitudinal atrophy spread in lvPPA. Our results show that two partially distinct brain networks anchored to the left anterior angular and posterior superior temporal gyri epicenters were preferentially associated with sentence repetition and naming skills in lvPPA. Critically,

the strength of connectivity within these two networks in the neurologically-intact brain significantly predicted longitudinal atrophy progression in lvPPA. Taken together, our findings indicate that atrophy progression in lvPPA, starting from inferior parietal and temporoparietal junction regions, predominantly follows at least two partially nonoverlapping pathways, which may influence the heterogeneity in clinical presentation and prognosis.

KEYWORDS
Alzheimer's disease, cortical atrophy, intrinsic connectivity networks, logopenic variant, longitudinal study, primary progressive aphasia

1 | INTRODUCTION

Several studies of selective network vulnerability in neurodegenerative diseases have shown that misfolded proteins propagate transneuronally in a prion-like manner from most vulnerable regions (i.e., disease epicenter) to connected structures (Ahmed et al., 2014; Goedert et al., 2017; Iba et al., 2013; Liu et al., 2012; Prusiner, 1984; Zhou et al., 2012). This network-based neurodegeneration hypothesis has received support from animal studies (Clavaguera et al., 2009; de Calignon et al., 2012; Iba et al., 2013), as well as from an increasing number of human neuroimaging studies demonstrating that neurodegeneration spreads along predetermined large-scale neural networks of functionally and structurally connected regions that closely mirror the patterns of atrophy seen in distinct neurodegenerative syndromes (Cope et al., 2018; Franzmeier & Dyrba, 2017; Mandelli et al., 2016; Seeley et al., 2009; Vogel et al., 2020; Zhou et al., 2010).

Primary progressive aphasia (PPA) is a family of neurodegenerative syndromes characterized by a relatively isolated and progressive loss of speech and language abilities that occurs when either frontotemporal lobar degeneration (FTLD) or Alzheimer's disease (AD) pathology preferentially targets language-related brain networks. Within this family, three main variants have been described (Gorno-Tempini et al., 2011): (1) the non-fluent/agrammatic variant (nfvPPA), characterized by impaired motor speech and/or agrammatism, and most often associated with abnormal deposition of microtubule-associated protein tau (Josephs et al., 2006; Kertesz et al., 2005; Spinelli et al., 2017); (2) the semantic variant (svPPA), characterized by impaired naming and single word comprehension, and most often associated with abnormal deposition of transactive response DNA-binding protein of 43kD (TDP-43) (Davies et al., 2005; Marsel Mesulam et al., 2008; Snowden et al., 2007; Spinelli et al., 2017); and (3) the logopenic variant (lvPPA), characterized by impaired single-word retrieval in spontaneous speech and naming and impaired repetition of phrases and sentences, and most often caused by underlying AD pathology (Giannini et al., 2017; Grossman, 2010; Harris & Jones, 2014; Kirshner, 2012; Mesulam, 2008; Migliaccio et al., 2009; Rabinovici et al., 2008; Rohrer et al., 2012; Spinelli et al., 2017).

In line with the network-based neurodegeneration hypothesis, current neuroimaging evidence indicates that the loss of brain tissue (i.e., atrophy) in nfvPPA originates in the left posterior inferior frontal gyrus and spreads within the speech production network to the precentral gyrus and supplementary motor area, supramarginal gyrus, posterior temporal regions, and subcortical and insular regions (Mandelli et al., 2016). Damage to these regions has been shown to be associated with motor speech and syntactic impairments (García et al., 2022; Mandelli et al., 2014; Mandelli et al., 2018; Wilson, Dronkers, et al., 2010). In svPPA, atrophy-related changes start in the left anterior temporal lobe and spread within the semantic network to the ventral and medial temporal lobe, cingulate, insular, orbitofrontal cortex, and angular gyrus (Brambati et al., 2009; Brown et al., 2019; Collins et al., 2017; Rosen et al., 2002). Damage to these regions has been previously associated with word comprehension and naming deficits (Chow et al., 2010; Cousins et al., 2016; Joubert et al., 2017; Migliaccio et al., 2016). On the other hand, in lvPPA, a few studies have revealed substantial variability regarding the location and extent of early atrophy, which often includes a large region comprising the left posterior temporal and inferior parietal cortices known to be susceptible to tau deposition and neurodegeneration in AD (Conca et al., 2022; Gorno-Tempini et al., 2008; Migliaccio et al., 2009; Ossenkoppele et al., 2016; Rohrer et al., 2013; Whitwell et al., 2019). Crucially, the lack of a well-defined epicenter in lvPPA hinders the mapping of specific networks related to lvPPA symptomatology and disease progression. This inconsistency across prior studies might, at least in part, be related to differences in methodology (volumetric studies or studies addressing cortical thickness or metabolic changes), the choice of anatomical parcellation atlases, and different nomenclature adopted by different investigators to describe brain regions in and around the left temporoparietal junction (TPJ) (Gorno-Tempini et al., 2008; Migliaccio et al., 2009; Phillips et al., 2018; Rohrer et al., 2013; Rogalski et al., 2016). Moreover, recent studies show that atrophy in lvPPA-related regions may underlie non-linguistic symptoms in lvPPA, such as deficits in attention and visuospatial functions (Ramanan et al., 2022), leaving open the question of which specific epicenters and associated networks are relevant for naming and repetition deficits, the two core aphasic symptoms in lvPPA. Therefore, the precise localization of early atrophy and its progression remains to be established. This information is also critical for tracking longitudinal changes in clinical trials and specifying potential target brain regions for brain stimulation in therapeutic trials (tDCS and TMS) (Ficek

et al., 2018; Gervits et al., 2016; Nissim et al., 2020; Tsapkini et al., 2018).

In this study, we performed a cross-sectional and longitudinal multimodal MRI investigation in a large cohort of well-characterized individuals with lvPPA and healthy controls. By leveraging an anatomically fine-grained atlas, we sought to improve the localization of early changes in cortical thickness in lvPPA, map the functional networks anchored to these regions in healthy controls, and test whether the strength of functional connectivity in language-relevant networks derived from the neurologically intact brain predicts longitudinal atrophy spread in lvPPA.

2 | MATERIALS AND METHODS

2.1 | Participants

From the database of the Memory and Aging Center at the University of California, San Francisco (UCSF-MAC), we selected individuals who had (i) an imaging-supported diagnosis of lvPPA according to published international criteria (Gorno-Tempini et al., 2011), (ii) a high-resolution structural 3D-T1 MRI scan that passed quality check, and (iii) a Mini-Mental State Examination (MMSE) score ≥15 and a Clinical Dementia Rating (CDR) <2. A total of 91 individuals with lvPPA were identified, and among them, 48 had a PET scan with ^{11}C-Pittsburgh Compound B (PIB, for amyloid-β pathology) and 22 had autopsy-proven pathology (of which 8 had a PIB-PET scan). One out of 48 had a negative PIB-PET scan, while 4 out of 22 had mixed or non-AD pathology. These participants were excluded from the study. Within the total cohort, we then isolated two nonoverlapping groups that had either a positive PIB-PET scan or autopsy-proven AD pathology as follows: (1) a group for the cross-sectional analysis ($lvPPA_{mild}$, $n = 15$; all of them had a positive PIB-PET scan and one had, in addition, autopsy-proven AD pathology) with a milder clinical presentation (MMSE >20 and CDR <1); (2) a group for the longitudinal analysis ($lvPPA_{long}$, $n = 28$; 24 had a positive PIB-PET scan; 13 had autopsy-proven AD pathology; 7 had both) with two MRI scans at least 1 year apart.

Three distinct groups of cognitively and neurologically intact individuals were also selected: (1) a group for the cross-sectional analysis (HC_{cross}, $n = 68$) matched to the $lvPPA_{tot}$ group for age, sex, handedness, education, and scanner type; (2) a group for the longitudinal analysis (HC_{long}, $n = 56$) matched to the $lvPPA_{long}$ group for age, sex, handedness, education, and scanner type; and (3) a group of individuals (HC_{conn}, $n = 50$) with resting-state functional MRI (rsfMRI) data for the delineation of the healthy intrinsic connectivity networks (ICNs).

All individuals with lvPPA underwent a comprehensive evaluation, including neurological history and examination, neuropsychological assessment (Kramer et al., 2003), and speech and language testing (Gorno-Tempini et al., 2004; Wilson, Henry, et al., 2010). Written informed consent was obtained from all participants or their surrogates. The study was approved by the University of California (San Francisco and Berkeley) and Lawrence Berkeley National Laboratory (LBNL) institutional review boards for human research.

2.2 | Image acquisition and processing

2.2.1 | PET imaging

Amyloid PET scans were acquired using ^{11}C-Pittsburgh compound B at LBNL on either a Siemens ECAT Exact HR PET only scanner ($n = 18$) or a Siemens Biograph 6 Truepoint PET/CT scanner ($n = 30$), as previously described (Villeneuve et al., 2015). PIB was synthesized and radiolabeled at LBNL's Biomedical Isotope Facility. Attenuation correction was performed using an emission scan (ECAT scanner) or a low-dose CT scan (Biograph scanner) acquired prior to PET acquisition. PET data were acquired in list mode and reconstructed using an ordered subset expectation maximization algorithm with weighted attenuation and smoothed with a 4 mm Gaussian kernel with scatter correction. PIB Standardized Uptake Value Ratio (SUVR) images were based on mean uptake over 50–70 min postinjection of ∼15 mCi of PIB (four 5-min frames).

PET frames were realigned, averaged and co-registered onto their corresponding structural MRI. PIB SUVR images were created in native space using the MRI-defined cerebellar gray matter as a reference region (Villeneuve et al., 2015). PIB-PET positivity was based on both visual reading, as validated against autopsy findings (La Joie et al., 2019; Lesman-Segev et al., 2020), and a quantitative analysis of the PIB-PET data. Briefly, the average PIB-SUVR is extracted from a large neocortical region of interest (ROI); resulting values are considered positive when exceeding a threshold of 1.21 (Villeneuve et al., 2015).

2.2.2 | Structural MRI

All brain structural MRI scans were acquired with either a 1.5 T Vision, 3 T Trio or 3 T Prisma scanner (Siemens Healthcare). For the longitudinal scans, we only included those collected using the same scanner at both time points. All the structural images were acquired with a T1-weighted 3D magnetization prepared rapid acquisition gradient echo sequence with the following parameters: 164 coronal slices; voxel size = 1.0 × 1.5 × 1.0 mm^3; FoV = 256 × 256 mm^2; matrix size = 256 × 256; TR = 10 ms; TE = 4 ms; T1 = 300 ms; flip angle = 15° (1.5 T); 160 sagittal slices; voxel size = 1.0 × 1.0 × 1.0 mm^3; FoV = 256 × 256 mm^2; matrix size = 256 × 256; TR = 2300 ms; TE = 2.98 ms for 3 T Trio and TE = 2.9 ms for 3 T Prisma; flip angle = 9° (3 T).

All T1-weighted images were first visually assessed to ensure the absence of artifacts or excessive motion. The images were processed through the Computational Anatomy Toolbox (CAT12; http://dbm.neuro.uni-jena.de/cat, version 12.7) with the Statistical Parametric Mapping software (SPM12; http://www.fil.ion.ucl.ac.uk/spm/software/spm12) running under MATLAB 2020b (http://www.mathworks.com).

The whole process consists of three steps: (1) an initial voxel-based processing, (2) a main voxel-based processing, and (3) a surface-based processing. In step (1), the images undergo a spatial adaptive nonlocal means denoising filter (Manjón et al., 2010). After bias correction and affine registration, the data undergo standard SPM unified segmentation (Ashburner & Friston, 2005). In step (2), the output images were skull-stripped and the brain parcellated into left and right hemisphere, subcortical regions and cerebellum. All the segmented tissue classes underwent a local intensity transformation before the final adaptive maximum a posteriori segmentation (Rajapakse et al., 1997), which is refined by applying a partial volume (Tohka et al., 2004). Finally, the segmented images were spatially normalized to a common reference space using the geodesic shooting registration (Ashburner & Friston, 2011). For the longitudinal data, the images were realigned from the two time points using inverse-consistent rigid-body registrations and intra-subject bias field corrections were applied (Ashburner & Ridgway, 2012; Reuter et al., 2012; Reuter & Fischl, 2011), thus assuring comparability across the time points. For the spatial registration to the reference brain template, a mean transformation for the time points was calculated and applied to all individual images. The use of an unbiased average image reduces random variations in the processing procedure and improves the robustness and sensitivity of the longitudinal analysis. In step (3), cortical thickness estimation and reconstruction of the central surface took place using a projection-based thickness method (Dahnke et al., 2013). After the initial surface reconstruction, topological defects were repaired using spherical harmonics (Yotter et al., 2010), and the final result is a central surface mesh that provides the basis for extracting folding patterns where the resulting local values were projected onto each node. Finally, the individual central surfaces were spatially registered to an average template using a spherical mapping (Yotter et al., 2011). Cortical thickness values were extracted using the HCP-MMP1.0 (Human Connectome Project [HCP] Multi-Modal Parcellation version 1.0) parcellation. This atlas was generated using multimodal brain images and an objective semi-automated neuroanatomical approach under the HCP (http://www.humanconnectomeproject.org/) and provides a fine-grained parcellation of the human brain into a total of 360 regions (180 per hemisphere). For a detailed description of parcellation nomenclature, we refer the reader to the neuroanatomical supplementary information provided in Glasser et al. (2016).

2.2.3 | Functional imaging processing

RsfMRI data were acquired on the 3 T Prisma scanner equipped with a 64-channel head coil and using a T2*-weighted multiband-EPI pulse sequence including 560 volumes with 66 AC/PC-aligned axial slices in interleaved order (slice thickness = 2.2 mm; in-plane resolution = 2.2 × 2.2 mm^2; FoV = 211 × 211 mm^2; TR = 850 ms; TE = 32.80 ms; flip angle = 45°; multiband factor of 6). The participants were asked to lie still in the scanner with eyes closed, remain awake and think of nothing. RsfMRI data were visually checked for quality control and only participants with a maximum relative head motion less than 2 mm for translation and 3 degrees for rotation were included. A total of 50 healthy controls matched by age and sex to the lvPPA group were included in the study (HC_{conn}, $n = 50$). Data were analyzed using an in-house pipeline combining different tools from FSL (http://fsl.fmrib.ox.ac.uk/fsl/fslwiki/), AFNI (http://afni.nimh.nih.gov/afni/), SPM (https://www.fil.ion.ucl.ac.uk/spm/software/spm12/), and ANTs (https://www.nitrc.org/projects/ants). The pre-processing steps involved slice timing correction and realignment of the functional whole-brain volumes, after discarding the first five volumes. Susceptibility-induced distortions, characteristic of EPI acquisitions, were estimated and corrected using the TOPUP tool (https://fsl.fmrib.ox.ac.uk/fsl/fslwiki/topup), which makes use of two additional spin-echo images acquired with opposing polarities of the phase-encode blips. The mean functional image was subsequently normalized to the MNI template using a combination of rigid, linear, and nonlinear warping, as implemented in ANTs. The independent component analysis (ICA)-AROMA tool was then utilized to identify and remove motion-related components from rsfMRI data in a data-driven fashion by means of an ICA (Pruim et al., 2015). Finally, time-series were band-pass filtered and CSF and WM mean signals were regressed out from the data and finally smoothed with an isotropic Gaussian kernel of 5 mm.

2.3 | Statistical analyses

The analyses aim to identify which of the anatomically parcellated regions are involved in mild lvPPA (epicenters), map the functional networks anchored to these regions in healthy controls, and identify which of the language-relevant networks are related to disease progression in lvPPA.

In this section, we describe in detail the steps used to (1) convert cortical thickness values in each region of the atlas to the W-score scale, (2) identify the regions of peak atrophy in the mild cohort of lvPPA, (3) derive the ICNs in the healthy individuals using the most atrophic regions from the analysis performed in 2.3.2 as seeds, (4) determine the ICNs most relevant to lvPPA symptomatology, (5) assess the cortical thickness change for each regions in the longitudinal cohort of lvPPA, and (6) test if the behaviorally relevant networks were significant predictors of atrophy progression in lvPPA. Finally, additional statistical analyses of behavioral data were performed using independent and paired *t* tests on the measures of dementia severity and language performance available in the participants both cross sectionally and longitudinally.

2.3.1 | Conversion of cortical thickness values to W-score scale

For each participant, mean cortical thickness values were extracted and covariate-adjusted on an ROI-by-ROI basis using the brain parcellation of the HCP-MMP1.0 atlas. Specifically, the influence of age, sex, handedness, and scanner type on cortical thickness was covaried

out by fitting a multiple regression model to the data from the group of healthy controls (HC_{cross}). Covariate-adjusted cortical thickness values (i.e., W-scores) were calculated for each ROI as follows: (observed cortical thickness − expected cortical thickness)/standard deviation of the residuals for that ROI in the healthy controls.

2.3.2 | Definition of the most vulnerable regions in the mild lvPPA cohort

Cross-sectional cortical thickness values on the W-score scale were modeled using ROI-specific simple linear regression models with the main effect of diagnostic status to identify the regions with the most significant cortical atrophy in the mild cohort of lvPPA ($lvPPA_{mild}$, $n = 15$) compared to the matched group of healthy controls (HC_{cross}, $n = 68$). Structural and metabolic studies have consistently shown that the left inferior parietal and TPJ are regions particularly vulnerable to neurodegeneration in lvPPA (Conca et al., 2022). Therefore, we predicted that a significant disease epicenter (i.e., a cluster of atrophic regions) would be identified within the left temporo-parietal cortex. In addition, since the size of the patient cohort used to identify the most atrophic regions was small ($n = 15$), we repeated the same analysis using the baseline MRI scans from the longitudinal and total cohorts of lvPPA patients ($n = 28$ and $n = 86$, respectively) to assess the reproducibility and generalizability of the results.

2.3.3 | ICN maps in healthy controls

The ICN maps were obtained by performing a seed-to-voxel analysis across the whole brain in the HC_{conn} ($n = 50$) group using the regions with the most significant difference between groups ($lvPPA_{mild}$ $n = 15$ vs. HC_{cross} $n = 68$) as seeds. For each of these seed regions, the average time series was extracted and used to compute the temporal correlation against all other voxels with a Pearson's r coefficient. Correlation coefficients were then converted to Z-scores by Fisher's r-to-Z transformation and group-level functional connectivity maps were derived by performing one-sample *t* tests in SPM12 with the null hypothesis set to zero and only positive correlations being tested. In order to enhance the robustness of the results and minimize the risk of false positives, we adopted a more stringent statistical threshold of $p < .001$, family wise error (FWE) corrected. Binary masks of each thresholded functional network were then created. For each functional network, regions from the HCP-MMP1.0 parcellation with at least 70% of overlap with the corresponding binary mask were considered part of that network.

2.3.4 | Identification of language-relevant ICNs in lvPPA

In order to ascertain the behavioral relevance of the ICNs in relation to the core language deficits in lvPPA, we performed a correlation analysis (involving the full cohort of 86 individuals with lvPPA) between atrophy (average W-score) within each of the networks and severity of the two defining clinical symptoms of lvPPA: impaired sentence repetition and confrontation naming (Gorno-Tempini et al., 2011). Specifically, we calculated the mean cortical thickness within each ICN in the total cohort of lvPPA ($n = 86$) as the average of W-scores (see Section 2.3.1) across all regions belonging to that ICN (see Section 2.3.3). We then derived one behavioral index of sentence repetition ability and another one of confrontation naming ability based on the six most difficult sentences from the Western Aphasia Battery (WAB) Repetition subtest (Kertesz, 1980) and Boston Naming Test (BNT; Kaplan et al., 1983), respectively. Repetition and naming are both tasks that involve language production. Therefore, in order to isolate task components preferentially related to auditory-verbal short-term memory (in sentence repetition) or lexical retrieval (in confrontation naming), we conducted partial correlation analyses (focusing on one variable while accounting for the other). Based on previous studies, we hypothesized that regions anchored to the TPJ would show stronger association with sentence repetition (Hickok & Poeppel, 2004), while the network connected to one or more subregions of the angular gyrus would be preferentially involved in lexical retrieval (Battistella et al., 2020).

2.3.5 | Identification of regions that demonstrate longitudinal atrophy-related changes in lvPPA

Cortical thickness values for each ROI in each participant with longitudinal data ($lvPPA_{long}$ $n = 28$) were converted into W-scores as described above in Section 2.3.1. Longitudinal trajectories of cortical thickness values on the W-score scale were modeled using ROI-specific linear mixed models with main effects for diagnostic status, time (defined as months since the first scan), and the two-way interaction of diagnostic status and time. Subject-specific random intercepts were included to account for dependencies due to repeated observations within participants. For each ROI, the interaction term between diagnostic status and time captures differences in the longitudinal trajectory of cortical atrophy between diagnostic groups over the study period. The corresponding t-statistic for the interaction term was treated as an index of the difference in cortical thickness change between the two diagnostic groups over time for each ROI defined in the parcellation atlas.

2.3.6 | Assessment of atrophy progression within the ICNs most relevant to the core language symptoms in lvPPA

By resorting to graph theoretical analysis, we calculated the shortest functional path from every ROI of the atlas parcellation to the seed-ROI of each ICN that showed an association with sentence repetition or naming deficits, which are the two defining symptoms of lvPPA (see Section 2.3.4). We then used this metric (shortest functional path

obtained from the healthy control group, $n = 50$) as a predictor of a region's degree of longitudinal atrophy progression in individuals with lvPPA ($n = 28$) (i.e., t-statistic from Section 2.3.5) as previously reported (Brown et al., 2019; Mandelli et al., 2016; Zhou et al., 2012). The inputs to the graph theory analysis were the regions of the HCP-MMP1.0 atlas (as nodes) and the Z-scores between pair of regions (as edges). The shortest functional path was calculated for each ROI as the sum of the edge weights forming the shortest path from a given ROI to the seed (Rubinov & Sporns, 2010) using an un-thresholded connectivity matrix in the Brain Connectivity Toolbox (BCT, https://www.nitrc.org/projects/bct). Following the network-based neurodegeneration hypothesis (Brown et al., 2019; Mandelli et al., 2016; Seeley et al., 2009; Zhou et al., 2010), a shorter path to the epicenter was expected to be associated with greater longitudinal cortical change. Multiple regression analyses were performed on the t-statistic for the interaction term of the cortical change for each ROI between the two diagnostic groups over time (see Section 2.3.5) and the shortest path length to the seed ROI. The Euclidean distance between the center of mass of each ROI and the epicenter of each ICN of interest was also calculated and included in the statistical analysis to account for the spatial proximity between each region and the seed.

We chose the salience network as a control network, as it is not usually involved in lvPPA. The salience network is composed of the anterior insula, dorsal anterior cingulate cortex, and frontoparietal operculum, and has been previously implicated in detecting and filtering important sensory, emotional, and cognitive information (Seeley et al., 2007). The salience network was seeded from the right anterior insula (right anterior agranular insula complex in the HCP-MMP1.0 atlas) using the same cohort of healthy controls ($n = 50$).

2.3.7 | Behavioral statistical analyses

Independent *t* tests and paired *t* tests were performed in the cross-sectional and longitudinal groups of lvPPA for MMSE, CDR sum of boxes, and language tasks to detect differences from the cognitively normal performance and longitudinal changes over the study period, respectively. Independent *t* tests were also performed between the mild group of lvPPA patients and the remaining lvPPA patients ($n = 71$) in order to highlight differences in symptom severity (see Table 1). When departures from normality of the data were detected, nonparametric alternatives were adopted.

3 | RESULTS

3.1 | Participants and clinical observation

Demographic and clinical data of the total cohort of individuals with lvPPA ($lvPPA_{tot}$, $n = 86$) are summarized in Table 1. This table also includes a description of the subgroup of individuals with mild symptoms ($lvPPA_{mild}$, $n = 15$) as well as the healthy control group used for the cross-sectional analysis (HC_{cross}, $n = 68$). Both the total cohort of lvPPA and the mild group exhibited the typical profile of impairment in verbal short-term memory (WAB repetition, digit span forward and California Verbal Learning Test [CVLT] trials 1–4) and confrontation naming when compared to healthy controls. Relative to the $lvPPA_{mild}$ group, the $lvPPA_{tot}$ group generally showed more severe impairment in overall cognition (lower MMSE and higher CDR scores) as well as language production (BNT, repetition, phonemic fluency), CVLT trials 1–4, and digit span backward. The total cohort of lvPPA encompasses the entire spectrum of impairment including the mild group. The statistical comparisons are indicated in Table 1.

Table 2 provides the summary demographic and clinical information for the two cohorts with longitudinal structural MRI data ($lvPPA_{long}$, $n = 28$; HC_{long}, $n = 56$). Paired *t* tests performed in the $lvPPA_{long}$ group showed longitudinal worsening of overall cognition (MMSE/CDR), core lvPPA symptoms (verbal short-term memory and naming) and decline of additional language skills (verbal fluency, single-word comprehension and sentence comprehension). With the exception of verbal episodic memory and arithmetic abilities, other cognitive domains, such as visual episodic memory, executive functioning, visuospatial, and visuo-constructive abilities, did not decline significantly between the two time points. This indicates that the progression of cognitive decline between the two time points within this cohort of patients was mostly restricted to the language domain, while other cognitive domains remained relatively stable across time.

3.2 | Specific anatomical regions in the left TPJ showed the greatest cortical atrophy in mild lvPPA

The cross-sectional comparison between the cohort of mild lvPPA ($lvPPA_{mild}$) and the matched group of healthy controls (HC_{cross}) yielded the typical asymmetric pattern of atrophy, with the left hemisphere showing more significant involvement than the right. Specifically, significant atrophy was observed in the left inferior parietal lobule and the TPJ, as well as the left lateral temporal cortex, dorsolateral prefrontal cortex, and posterior cingulate cortex. Figure 1 illustrates a surface rendering of the atrophy pattern in the mild cohort of lvPPA ($n = 15$), along with the total cohort of lvPPA ($n = 86$) and the baseline atrophy of the longitudinal cohort ($n = 28$) (see Supplementary Table 1 for statistical details). Notably, the left inferior parietal region showed the greatest atrophy across all three lvPPA cohorts, particularly in the left anterior part of the angular gyrus corresponding to the parietal area F, part m (PFm) of the HCP-MMP1.0 parcellation. Significantly and consistently atrophic brain regions were also detected in the left middle frontal gyrus as well as the superior and middle temporal cortices.

In this context, we defined as putative epicenters the regions that were (i) associated with the highest *p*-value and (ii) spatially clustered together within the left temporo-parietal cortex. According to the

TABLE 1 Summary of demographic and cognitive profiles for the individuals with lvPPA and healthy controls used for the cross-sectional analysis.

	$lvPPA_{tot}$	$lvPPA_{mild}$	HC_{cross}
n	86	15	68
Demographics			
Age, mean (years)	64.3 ± 8.2	62.2 ± 6.8	65.6 ± 8.8
Education, mean (years)	16.7 ± 2.9	16.8 ± 2.5	17.4 ± 2.0
Sex, *n* female (%)	44 (51.2)	5 (33.3)	36 (53.0)
Handedness, *n* right (%)	72 (85.7)	13 (86.7)	60 (89.5)
Biomarker-confirmed AD (%)	65	100	NA
Disease severity			
Symptom onset, mean (years)	59.4 ± 8.0	57.1 ± 6.4	N/A
MMSE (30)	20.4 ± 6.6[a,b]	24.1 ± 3.9[a]	29.3 ± 0.9
CDR global (3)	0.6 ± 0.4[a,b]	0.5 ± 0.1[a]	0.0 ± 0.0
CDR sum of boxes (18)	3.4 ± 2.1[a]	2.6 ± 0.9[a]	0.0 ± 0.0
Language production			
Boston (object) Naming Test (15)	9.3 ± 4.2[a,b]	11.8 ± 3.4[a]	14.6 ± 0.8
WAB sentence 10–15 items (66)	39.4 ± 12.3[b,c]	46.0 ± 7.6[c]	65.0 ± 1.0[ND]
WAB Repetition Total (100)	72.4 ± 14.2[b,c]	79.4 ± 7.8[c]	99.0 ± 1.0[ND]
Phonemic (D-letter) fluency	7.5 ± 4.5[a,b]	10.6 ± 4.1[a]	16.3 ± 5.1
Semantic (animals) fluency	8.9 ± 5.8[a,b]	11.8 ± 6.2[a]	23.3 ± 5.0
Language comprehension			
Syntax comprehension (%)	87.8 ± 13.4[c]	87.9 ± 8.2[c]	98.6 ± 1.8[ND]
PPVT (16)	13.7 ± 2.2[b,c]	14.9 ± 1.1	15.7 ± 0.6[ND]
Working memory and executive functions			
Digit span forward	4.2 ± 1.2[a]	4.4 ± 1.1[a]	6.8 ± 1.3
Digit span backward	2.9 ± 1.2[a,b]	3.7 ± 1.1[a]	5.4 ± 1.2
Calculations	3.1 ± 1.4[c]	3.1 ± 1.2[c]	5.0 ± 0.0[ND]
Design fluency: correct designs	6.1 ± 3.2[a]	6.6 ± 3.2[a]	11.4 ± 3.0
Modified trails: time (120 s)	87.3 ± 35.6[a]	75.1 ± 37.7[a]	24.6 ± 9.2
Modified trails: correct (14)	10.0 ± 5.3[a]	11.1 ± 4.6[a]	13.6 ± 2.4
Visuospatial function			
Benson figure copy (17)	13.2 ± 4.2[a]	13.9 ± 3.3[a]	15.4 ± 0.8
VOSP number location (10)	7.7 ± 2.3[a]	8.3 ± 1.9[a]	9.1 ± 1.0
Episodic memory			
Benson figure recall (17)	6.0 ± 4.0[a]	7.1 ± 3.3[a]	11.8 ± 2.6
CVLT trials 1–4 (40)	14.0 ± 7.4[b,c]	17.7 ± 7.1[c]	29.8 ± 3.4[ND]
CVLT 30 s free recall (10)	3.4 ± 2.7[c]	4.5 ± 2.7[c]	8.0 ± 1.1[ND]
CVLT 10 min free recall (10)	2.9 ± 2.9[c]	3.5 ± 3.1[c]	7.5 ± 1.3[ND]
CVLT recognition (9)	7.4 ± 1.7	7.7 ± 1.2	8.6 ± 0.7[ND]

Note: Due to the paucity of neuropsychological data from the HC cohort, normative data were used for eight scores, marked with [ND]: The WAB Repetition Total scores were derived from the WAB manual (Kertesz, 1980). The average score (% correct) for syntax comprehension was derived from a normative sample in our center published in Lukic et al. (2019). Average HC scores for the PPVT were derived from a normative sample in our center, published in Watson et al. (2018). The average scores for our four subscores of the CVLT and the calculations task were derived from a normative sample in our center, unpublished.

Abbreviations: CDR, Clinical Dementia Rating; CVLT, California Verbal Learning Test; DF, design fluency; HC, healthy control; MMSE, Mini-Mental State Examination; PPVT, Peabody Picture Vocabulary Test; VOSP, Visual Object and Space Perception; WAB, Western Aphasia Battery.

[a]Significantly different from HC at $p < .05$.

[b]Significantly different from other lvPPA cohort at $p < .05$.

[c]Scores fall 2 or more standard deviations below normative data means, where applicable.

TABLE 2 Summary of demographic and cognitive profiles for $lvPPA_{long}$ and HC_{long} cohorts across two time points.

Variable	$lvPPA_{long}$			HC_{long}		
	First timepoint	Second timepoint	*N* (first/second)	First timepoint	Second timepoint	*N* (first/second)
Overall *n*	**28**	**28**		**56**	**56**	
Demographics						
Age (years)	64.2 ± 8.3	65.3 ± 8.2[a]	28/28	61.6 ± 7.9	62.7 ± 8.1	56/56
Education, mean (years)	17.21 ± 3.28	17.21 ± 3.28	28/28	17.39 ± 2.29	17.39 ± 2.29	54/54
Sex, *n*, female (%)	16 (57.0)	16 (57.0)	28/28	34 (61.0)	34 (61.0)	56/56
MMSE (30)	23.3 ± 3.4[b]	19.2 ± 5.5[a,b]	28/23	29.5 ± 0.8	29.5 ± 1.2	55/42
CDR global (3)	0.6 ± 0.2[b]	0.7 ± 0.3[b]	28/28	0.0 ± 0.0	0.0 ± 0.0	44/42
CDR sum of boxes (18)	2.8 ± 1.4[b]	3.6 ± 1.8[a,b]	28/28	0.00 ± 0.1	0.0 ± 0.0	44/42
Language production						
Boston Naming Test (15)	11.0 ± 3.2[b]	8.7 ± 4.5[a,b]	28/22	14.6 ± 0.7	14.7 ± 0.7	51/39
WAB Fluency Rating (10)	8.3 ± 1.2[c]	7.9 ± 1.4[c]	26/23	10.0 ± 0.0 [ND]	10.0 ± 0.0 [ND]	N/A
WAB Repetition Total (100)	76.0 ± 9.3[c]	67.6 ± 15.2[a,c]	23/23	99.0 ± 1.0[ND]	99.0 ± 1.0[ND]	N/A
Phonemic (D-letter) fluency	8.0 ± 4.2[b]	4.7 ± 3.6[a,b]	28/23	16.8 ± 5.3	17.9 ± 4.8	44/39
Semantic (animals) fluency	10.8 ± 4.8[b]	7.3 ± 4.0[a,b]	28/23	24.6 ± 6.3	23.4 ± 5.5	51/28
Language comprehension						
Syntax comprehension (%)	91.0 ± 8.9[c]	78.1 ± 24.0[a,c]	20/14	98.6 ± 1.8[ND]	898.6 ± 1.8[ND]	N/A
PPVT (16)	14.5 ± 1.6[b]	13.4 ± 2.2[a,b]	24/21	15.9 ± 0.3	15.9 ± 0.3	29/25
Working memory and executive functions						
Digit span forward	4.5 ± 1.0[b]	3.9 ± 1.2[a,b]	28/23	7.0 ± 1.4	7.3 ± 1.2	35/23
Digit span backward	3.0 ± 0.8[b]	2.5 ± 0.9[a,b]	28/23	5.6 ± 1.4	5.8 ± 1.4	50/38
Calculations (5)	3.5 ± 1.0[b]	2.7 ± 1.2[a,b]	28/23	4.9 ± 0.4	4.9 ± 0.4	34/32
DF: correct designs	6.1 ± 3.1[b]	5.3 ± 3.4[b]	28/18	10.9 ± 2.9	11.8 ± 3.4	33/30
Modified trails: time (120 s)	90.1 ± 34.5[b]	88.5 ± 37.4[b]	27/21	22.6 ± 7.8	22.6 ± 10.0	51/41
Modified trails: correct (14)	10.4 ± 4.7[b]	9.4 ± 5.3[b]	27/21	13.3 ± 3.0	13.7 ± 2.2	51/41
Visuospatial function						
Benson figure copy (17)	14.9 ± 2.5	14.0 ± 2.8[b]	28/23	15.7 ± 0.9	15.8 ± 0.7	34/30
VOSP number location (10)	7.8 ± 1.9[b]	7.4 ± 2.9[b]	26/22	9.1 ± 1.7	9.1 ± 1.8	44/41
Episodic memory						
Benson figure recall (17)	7.5 ± 4.1[b]	6.0 ± 4.2[b]	28/23	12.8 ± 2.8	12.6 ± 3.0	34/30
CVLT (trials 1–4) correct (36)	16.4 ± 5.9[b]	12.8 ± 6.1[a,b]	27/23	31.3 ± 2.5	31.4 ± 2.9	19/5
CVLT (10-min) delay (9)	3.7 ± 3.1[b]	2.1 ± 2.3[a,b]	27/23	7.9 ± 1.4	8.8 ± 0.4	19/5
CVLT recognition (9)	7.9 ± 1.4	7.7 ± 1.6	27/23	8.7 ± 0.6	8.8 ± 0.4	19/5

Note: Due to the paucity of neuropsychological data from the two HC cohorts, normative data were used for three scores, marked with [ND]: The WAB fluency Rating and Repetition Total scores were derived from the WAB-R manual (Kertesz, 1980). The average score (% correct) for syntax comprehension was derived from a normative sample in our center published in Lukic et al. (2019).

Abbreviations: CDR, Clinical Dementia Rating; CVLT, California Verbal Learning Test; DF, design fluency; HC, healthy control; MMSE, Mini-Mental State Examination; [ND], normative data; PPVT, Peabody Picture Vocabulary Test; VOSP, Visual Object and Space Perception; WAB, Western Aphasia Battery.

[a]Significantly different for lvPPA from timepoint 1 to timepoint 2, per paired-samples *t* test.

[b]Significantly different from HC for the same timepoint at $p < .05$.

[c]Scores fall 2 or more standard deviations below normative data means, where applicable.

HCP-MMP1.0 brain parcellation, these regions correspond to the parietal area F, part m (PFm) (coefficient ± SE = −4.28 ± 0.34; $t = -12.6$, $p < .001$), to parietal area F (PF) (−3.58 ± 0.31; $t = -11.5$, $p < .001$), parietal area G inferior (PGi) (−3.30 ± 0.29; $t = -11.4$, $p < .001$), parietal area G superior (PGs) (−3.24 ± 0.32; $t = -10.2$, $p < .001$), intraparietal area 0 (IP0) (−2.79 ± 0.29; $t = -9.7$, $p < .001$), intraparietal area 2 (IP2) (−3.00 ± 0.32; $t = -9.5$, $p < .001$), and perisylvian language (PSL) area (−2.71 ± 0.28; $t = -9.7$, $p < .001$).

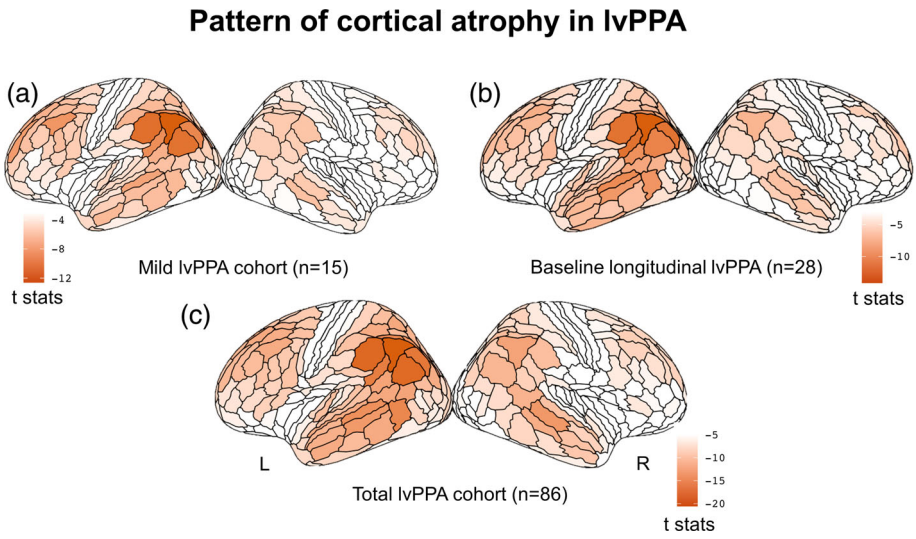

FIGURE 1 Cross-sectional pattern of cortical atrophy in logopenic variant of primary progressive aphasia (lvPPA) compared to HC. Surface rendering of the atrophy pattern in the mild cohort of lvPPA ($n = 15$) (a), at the baseline atrophy of the longitudinal cohort ($n = 28$) (b), and in the total cohort of lvPPA ($n = 86$). The render is performed with the ggseg toolbox in R (https://lcbc-uio.github.io/ggseg/) on the Glasser brain atlas. The left inferior parietal region showed the greatest atrophy across all three lvPPA cohorts.

3.3 | Two partially distinct ICNs were significantly associated with naming and repetition deficits in lvPPA

The seven left hemisphere regions identified in the previous analysis as the earliest and most atrophic regions in lvPPA (PFm, PF, PGi, PGs, IP0, IP2, and PSL) were used as seed-ROIs to extract the corresponding ICNs in the HC_{conn} cohort. In order to ascertain the behavioral relevance of these seven ICNs in relation to the core language deficits in lvPPA, we performed a correlation analysis (involving the full cohort of 86 individuals with lvPPA) between global atrophy (average W-score) within each of the networks (including only the label assigned to the network as indicated in Section 2.3.4) and the two defining clinical symptoms of lvPPA: impaired confrontation naming and sentence repetition. Due to the non-Gaussian distribution of the test scores (BNT $W = 0.93$, $p < .001$), we used Spearman's correlation. Given that repetition and naming scores were significantly correlated (Spearman's $rho = 0.52$, $p < .001$), we performed a one-tailed partial correlation analysis (we only expected to observe a positive relationship) between global atrophy (lower values indicate greater global atrophy) and performance (lower scores indicate worse performance) controlling for the influence of the other variable.

Repetition skills (controlling for naming scores) were only significantly correlated with atrophy in the PSL-ICN ($rho = 0.22$, $p = .03$) while naming skills (controlling for repetition scores) were only significantly correlated with atrophy in the PFm-ICN ($rho = 0.21$, $p = .03$). No other partial correlation reached statistical significance for any of the other networks. In Supplementary Figure 1, we show all the networks identified in the healthy controls and highlight the two networks most relevant to lvPPA symptomatology.

As described in Section 2, for subsequent analysis, we focused only on the two networks seeded in the left PFm and PSL, which resemble networks previously associated with the typical pattern of atrophy in lvPPA. The PFm network (Figure 2a) encompass areas within the inferior parietal and temporal gyri as well as the middle frontal gyrus and resembles the posterior component of the default mode network (DMN). The PSL network (Figure 2b) encompass areas within the superior and middle temporal gyri along with the lateral frontal pole and resembles the speech perception network (Battistella et al., 2020). As shown in Figure 2c, there is some degree of anatomical overlap between these two networks within the perisylvian region, a portion of the inferior temporal lobe and the precuneus. Overall, however, the nonoverlapping portions dominate.

3.4 | Longitudinal pattern of cortical atrophy in lvPPA

The longitudinal comparison between the $lvPPA_{long}$ and HC_{long} cohorts revealed that the most significant change in cortical thickness occurred bilaterally in the auditory lateral temporal cortices, the inferior parietal cortex (Figure 3), the posterior cingulate cortex as well as in the left inferior and middle frontal gyri. According to the HCP-MMP1.0 atlas, the regions that showed the greatest change were located in the dorsal portion of the right superior temporal sulcus (STSdp) (coefficient ± SE = −0.043 ± 0.006; $t = -7.4$, $p < .001$), followed by the left temporal area F (TF) (−0.044 ± 0.007; $t = -6.0$, $p < .001$), the right PGs (−0.043 ± 0.008; $t = -5.6$, $p < .001$), the right temporal–parietal–occipital junction area 1 (TPOj1) (−0.028 ± 0.005; $t = -5.5$, $p < .001$), the left dorsal 23 section a-b of the posterior cingulate gyrus (d23ab) (−0.035 ± 0.006; $t = -5.4$, $p < .001$), the left prostriate cortex (ProS) (−0.048 ± 0.009; $t = -5.3$, $p < .001$), the left PGi (−0.034 ± 0.007; $t = -5.2$, $p < .001$), and the ventral portion of the left superior temporal sulcus (STSvp) (−0.033 ± 0.007; $t = -5.0$, $p < .001$). All the regions along with their statistical significance are provided in Supplementary Table 2.

3.5 | The ICNs associated with sentence repetition and naming deficits were significant predictors of longitudinal atrophy progression in lvPPA

The multiple regression analyses performed between the shortest path length from each ROI to the seed region of each ICN and the ROI-specific t-statistic from the analysis of longitudinal change in

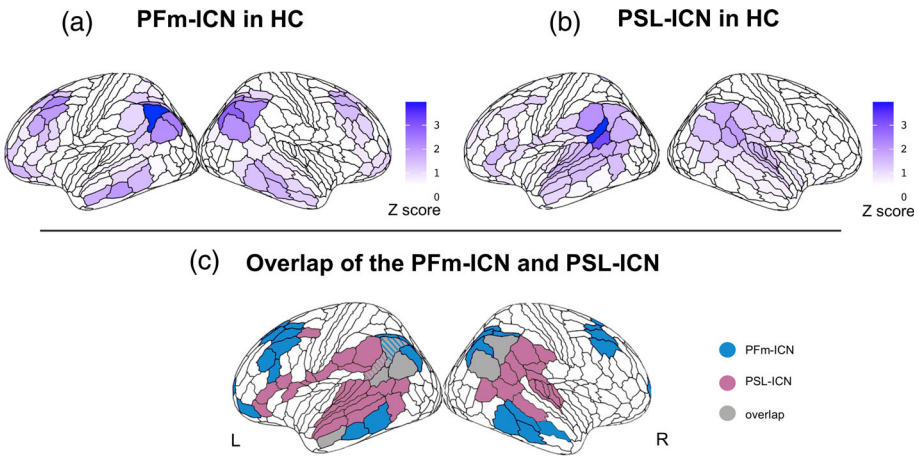

FIGURE 2 Two partially distinct intrinsic connectivity networks (ICNs) associated with naming and repetition deficits in logopenic variant of primary progressive aphasia (lvPPA). The intrinsic connectivity map (Z score) extracted from the HCconn cohort seeded in the left PFm (a) includes areas in the inferior parietal and temporal gyri and in the middle frontal gyrus. The intrinsic connectivity map (Z score) extracted from the HCconn cohort seeded in the left PSL (b) includes areas in the superior and middle temporal gyri and in the lateral frontal pole. The overlap between these two networks includes regions in the perisylvian region, the inferior temporal lobe, and the precuneus (c).

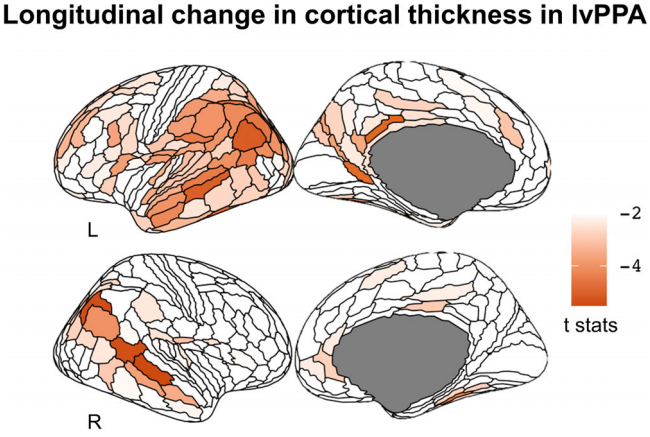

FIGURE 3 Longitudinal change in cortical thickness in the logopenic variant of primary progressive aphasia ($lvPPA_{long}$) cohort compared to matched health control (HC) with longitudinal data. The longitudinal change in cortical thickness occurred bilaterally in the auditory lateral temporal cortices, the inferior parietal cortex, in the posterior cingulate cortex, and in the left inferior and middle frontal gyri. The render is performed with the ggseg toolbox in R (https://lcbc-uio.github.io/ggseg/) on the Glasser brain atlas.

cortical thickness in lvPPA (controlling for Euclidian distance) yielded that the two ICNs, which were found to be selectively associated with sentence repetition and naming deficits, were also significant predictors of longitudinal atrophy progression in lvPPA: PFm-ICN ($r = .28$, $p < .001$) and PSL-ICN ($r = .21$, $p < .001$). In contrast, longitudinal atrophy progression in lvPPA was not predicted by the shortest path length to the seed region of the salience network (right anterior insula, used as a control network here). The corresponding scatterplots for the relationship between the shortest path length to the network epicenters left PFm, left PSL, right AICC, and the longitudinal change in cortical thickness (ROI-specific t-statistic) for each ROI of the HCP-MMP1.0 atlas in lvPPA are shown in Figure 4.

4 | DISCUSSION

In this cross-sectional and longitudinal multimodal MR imaging study, we showed that lvPPA aphasic symptomatology and longitudinal atrophy progression were associated with anatomical changes in partly overlapping functional networks anchored to two left temporo-parietal epicenters. These findings have important implications for improving the accuracy with which atrophy epicenters can be localized in diseases with a heterogeneous clinical presentation, such as lvPPA. Additionally, our results support the model of network-based neurodegeneration, where brain regions connected to disease epicenters are preferentially targeted by neurodegeneration, driving the symptomatology that characterizes each clinical syndrome. These insights can facilitate the development of evidence-based therapies and help to identify anatomically well-defined brain stimulation sites for therapeutic studies. Ultimately, our study contributes to a deeper understanding of the underlying mechanisms of neurodegenerative diseases and the heterogeneity in clinical presentation and progression in lvPPA.

4.1 | General pattern of atrophy and most vulnerable cortical regions in lvPPA

Consistent with prior studies, we confirmed an asymmetric pattern of atrophy in lvPPA characterized by the cortical involvement of left hemisphere structures including the inferior parietal lobe, the TPJ, the dorsolateral prefrontal cortex, the superior and middle temporal gyri and to a lesser extent, regions in the right inferior parietal lobe and in

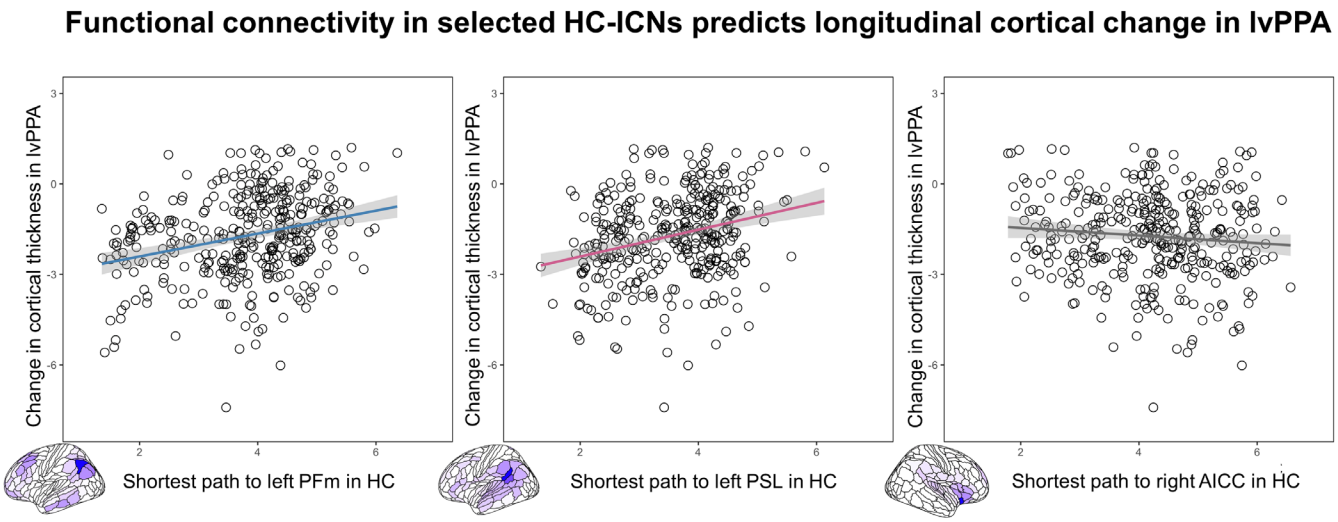

FIGURE 4 Functional connectivity in selected healthy control-intrinsic connectivity networks (HC-ICNs) predicts longitudinal cortical change in logopenic variant of primary progressive aphasia (lvPPA). Scatterplots of the correlation between the shortest functional path length from the left PFm, perisylvian language (PSL), and right AICC in the HC group and the longitudinal change in cortical thickness in lvPPA. On the scatterplot, each dot represents the statistical change in cortical thickness in each region of the HCP-MMP1.0 atlas.

the right middle temporal and frontal gyri (Giannini et al., 2017; Gorno-Tempini et al., 2004; Henry & Gorno-Tempini, 2010; Mesulam et al., 2009; Phillips et al., 2018; Preiß et al., 2019; Rogalski, Cobia, Harrison, Wieneke, Thompson, et al., 2011; Rogalski, Cobia, Harrison, Wieneke, Weintraub, & Mesulam, 2011; Teichmann et al., 2013). In particular, using a surface-based approach paired with a fine-grained brain parcellation of the cerebral cortex, we localized the most significant atrophy within the left inferior parietal lobe and the posterior-superior tip of the Sylvian fissure at the TPJ. While most voxel-based morphometry studies have found atrophy encompassing the middle and superior temporal gyri, it is noteworthy that the most consistently hypometabolic region across PET studies of lvPPA falls in the left inferior parietal lobe (Conca et al., 2022). Interestingly, in our study, the most atrophic peak was located in the left anterior portion of the angular gyrus (PFm), a region that has been described as a transitional area based on its cytoarchitectonic features (Caspers et al., 2006, 2008). The same pattern was observed in the longitudinal lvPPA cohort (using baseline MRI scans) as well as in the larger lvPPA cohort, which spanned a wider range of disease severity. Taken together, these findings indicate that, at the group level, the pattern of brain atrophy is consistent across groups, multifocal, and centered around specific anatomical loci within the left inferior parietal lobe and the TPJ (Gorno-Tempini et al., 2011).

Methodological differences might partially explain why accurate identification of early atrophy loci in lvPPA has been problematic. Previous neuroimaging studies typically used standard voxel-based analysis or surface-based approaches coupled with coarse brain atlases, preventing precise localization of early atrophic regions in lvPPA. Different nomenclature in and around the inferior parietal regions and TPJ may also contribute to the lack of consistency across studies. In this study, we applied a surface-based approach to structural T1-weighted MR images combined with a recent, more anatomically fine-grained brain parcellation atlas that captures the multimodal fingerprint of each cortical area (Glasser et al., 2016). Critically, compared to voxel-based analyses, surface-based methods have been shown to be most sensitive in capturing atrophy of the cortical ribbon (Diaz-de-Grenu et al., 2014), especially in the parietal lobe, which is characterized by a thinner cortical sheet compared to the temporal lobe (Hogstrom et al., 2013). Indeed, our findings improve neuroanatomical precision by mapping putative atrophy epicenters to a detailed parcellation of cortical areas bounded by sharp changes in architecture, function, connectivity, and/or topography.

4.2 | Brain networks associated with the core language symptoms of lvPPA

After identifying the specific anatomical location of the most vulnerable regions within the left temporo-parietal cortex in individuals with lvPPA, we used these loci as seed ROIs to delineate their corresponding functional ICNs in healthy individuals and to investigate the behavioral relevance of these networks for the core symptomatology of lvPPA (i.e., impaired sentence repetition and confrontation naming abilities). By employing brain–behavior correlation analyses to evaluate the relation between the structural integrity of each ICN identified in the healthy brain and these core symptoms of lvPPA, we were able to isolate two behaviorally relevant networks: one anchored in the left PFm, which was preferentially associated with auditory–verbal short-term memory (sentence repetition) and one in the left PSL, which was implicated in lexical retrieval (confrontation naming). The two ICNs identified in this study as preferentially involved in sentence repetition and confrontation naming are consistent with findings from previous literature in post-stroke aphasia, functional imaging in healthy controls, and PPA (Forkel et al., 2020; Fridriksson et al., 2010; Miller et al., 2021; Rogalsky

et al., 2015). Specifically, language production skills have been linked to a large-scale network involving frontal-temporal–parietal regions (Gleichgerrcht et al., 2015; Indefrey & Levelt, 2004; Mesulam et al., 2014; Migliaccio et al., 2016; Milton et al., 2021) with the left angular gyrus (including PFm) being specifically associated with impaired confrontation naming (DeLeon et al., 2007) and the TPJ (including PSL) with repetition skills (Baldo et al., 2012; Buchsbaum & D'Esposito, 2009; Lukic et al., 2019; Majerus, 2013).

Interestingly, previous rsfMRI studies were not able to identify a single, one-to-one mapping between the atrophy pattern in lvPPA and a unique functional network related to clinical symptoms and/or disease (Battistella et al., 2020; Lehmann, Ghosh, et al., 2013; Lehmann, Madison, et al., 2013; Ossenkoppele et al., 2015). When considering language-related networks, Battistella et al., 2020 found that lvPPA was the only PPA variant not associated with one specific functional network. Similarly, studies that considered lvPPA and other AD clinical phenotypes (Lehmann, Ghosh, et al., 2013; Lehmann, Madison, et al., 2013; Ossenkoppele et al., 2015) found an overlap between the lvPPA atrophy pattern and the posterior DMN (middle temporal gyrus, inferior parietal lobule, and posterior cingulate cortex) as well as "off-DMN" regions (left superior and inferior temporal cortex). Our analysis, by further partitioning the networks previously considered, revealed an association between specific network subcomponents and the most relevant clinical symptoms in lvPPA. Therefore, the observations from the present study, in combination with prior evidence, supports the notion that the multifaceted linguistic and cognitive profile of lvPPA might arise from a neurodegenerative process that preferentially targets networks subcomponents, potentially explaining the difficulties in defining this variant as a unitary clinical syndrome (Hu et al., 2010; Machulda et al., 2013; Leyton et al., 2015; Louwersheimer et al., 2016; Ramanan et al., 2022; Sajjadi et al., 2012). Future studies might leverage these findings to better understand heterogeneity in the clinical presentation and progression of lvPPA and other atypical AD clinical phenotypes.

4.3 | Brain networks associated with naming and repetition predict atrophy progression in lvPPA

The results of our longitudinal analysis of cortical thickness changes are in line with previous reports showing marked progression of atrophy over time in lvPPA within functional networks anchored to syndrome-specific, behaviorally relevant epicenters. According to prior studies, atrophy remains asymmetrical in temporo-parietal regions (left > right) despite significant bilateral involvement (Rogalski, Cobia, Harrison, Wieneke, Thompson, et al., 2011; Rogalski, Cobia, Harrison, Wieneke, Weintraub, & Mesulam, 2011; Rohrer et al., 2013). In our study, the most prominent longitudinal atrophy change was observed bilaterally in temporo-parietal regions that were also involved in mildly impaired lvPPA patients but to a lesser extent, thus showing the most marked change. Critically, we found that the longitudinal spread of atrophy was significantly predicted by the estimated (in healthy controls) length of the shortest functional path to the epicenter of the two networks associated with the two core language symptoms of lvPPA. Informed by the network-based neurodegeneration hypothesis, we anticipated that the greatest cortical thinning over time would occur primarily in the regions that show the strongest functional connectivity with the disease epicenter (the initial peak of atrophy). Indeed, we confirmed that the brain network anchored in the most atrophic region in lvPPA (PFm) was behaviorally relevant (associated with lvPPA symptomatology) and predicted longitudinal atrophy spread. This functional brain network appears to overlap with the DMN that has previously been implicated in AD pathology (Buckner, 2004; Greicius et al., 2004). Less expectedly, however, we found a second brain network anchored in a separate temporo-parietal area critical for language that was also involved in the spread of cortical atrophy in lvPPA. Therefore, these findings strongly indicate that more than one predefined large-scale functional system in the brain shapes the pattern of progression of cortical atrophy in lvPPA and drives its associated symptomatology.

Considering that we intentionally chose to select only individuals with lvPPA who had either a positive PIB-PET scan or autopsy-proven AD pathology as part of the longitudinal cohort, it seems sensible to assume that AD is very likely to be the primary underlying neuropathology driving the spread in our patients. In this context, it has been shown that amyloid-beta depositions are typically located in highly interconnected cortical regions (Buckner et al., 2009; Lehmann, Ghosh, et al., 2013; Lehmann, Madison, et al., 2013), which may facilitate the spread of AD pathology across functionally coupled networks compared to other pathologies that frequently underlie other PPA variants such as FTLD-tau or TDP (Spinelli et al., 2017). Therefore, it could be argued that the multifaceted nature of the core language symptoms in lvPPA with probable AD pathology may arise from the disruption of multiple, distinct functional networks. Although we could not directly investigate the relationship between longitudinal atrophy progression and decline in language abilities due to missing behavioral data, we did observe worsening of naming and repetition skills over time in lvPPA, with a slightly greater effect for naming than repetition which might be explained by the prominent longitudinal thinning of temporal areas bilaterally. Nonetheless, the verbal short-term memory deficit in our sample was clearly demonstrated by cross-sectional and longitudinal differences in digit span forward, in addition to WAB sentence repetition, providing additional support to theories that posit phonologic working memory dysfunction as a central feature of AD-associated PPA (Giannini et al., 2017; Gorno-Tempini et al., 2008). More direct evidence comes from a recent study of PPA patients (nfvPPA, svPPA, and lvPPA) with autopsy-confirmed AD pathology showing that the rate of decline in naming and repetition skills correlated with the pathological burden (quantified at the time of autopsy) in different left perisylvian regions (Cousins et al., 2021).

4.4 | Limitations of the study

We acknowledge several limitations of our study. The seed-ROI approach used in this study has the advantage of being more

interpretable and straightforward, but global analyses of network modularity are needed to better support any spatial distinction drawn between the two identified networks. While the use of the Euclidean distance for estimating spatial proximity is a widely adopted method, other distance metrics, such as geodesic distance along the cortical sheet or the length of deep white matter tracts, could provide a more accurate reflection of anatomical connectivity between regions. Furthermore, future studies with larger sample sizes or aggregated multicentric datasets, as well as comprehensive profiling of cognitive abilities (both verbal and nonverbal), will be necessary to assess the generalizability of our findings (including the replicability of putative disease epicenters), to determine the specific language functions subserved by these networks and to explore the potential existence of endophenotypes in lvPPA. Despite these limitations, our study provides valuable insights into the network anatomy of lvPPA and lays the groundwork for future research in this field.

5 | CONCLUSION

Taken together, these findings indicate that atrophy progression in lvPPA, starting from inferior parietal and TPJ regions, predominantly follows at least two partially distinct pathways, which are associated with auditory-verbal short-term memory and lexical retrieval skills. This indicates that more than one large-scale functional system in the brain influences the pattern of cortical atrophy progression in lvPPA and drives its associated symptomatology. This may help explain the heterogeneity in the clinical presentation and prognosis of individuals with lvPPA. By adopting a network-based perspective of neurodegenerative diseases, we have provided new insights into the network anatomy underpinning lvPPA, therefore advancing scientific knowledge of disease pathogenesis and providing new perspectives to inform future studies investigating the existence of varying endophenotypes in lvPPA.

ACKNOWLEDGMENT

The authors thank the participants and their families for the time and effort they dedicated to the research.

FUNDING INFORMATION

The study was supported by grants from the National Institutes of Health (NINDS R01 NS050915, NIA P50 AG03006, NIA P30 AG062422, NIA P01 AG019724, NIDCD R01DC016291, NIA K99AG065501); Alzheimer's Disease Research Centre of California (03–75271 DHS/ADP/ARCC); Larry L. Hillblom Foundation; John Douglas French Alzheimer's Foundation; Koret Family Foundation; Consortium for Frontotemporal Dementia Research; and McBean Family Foundation and a Career Scientist Award (NFD) from the US Department of Veterans Affairs Clinical Sciences R&D Program. These supporting sources had no involvement in the study design, collection, analysis or interpretation of data, nor were they involved in writing the paper or the decision to submit this report for publication. D.L.L-P. and A.G-V. were each supported by a postdoctoral fellowship from the Chilean National Agency for Research and Development (ANID BECAS-CHILE 74200073 and ANID BECAS-CHILE 74200065, respectively). D.L.L-P. is supported with funding from the Chilean National Agency for Research and Development (ANID SUBVENCIÓN A LA INSTALACIÓN EN LA ACADEMIA 85220006).

DATA AVAILABILITY STATEMENT

While we can share anonymized data, public archiving is not yet permitted under the study's IRB approval due to the sensitive nature of the data. Specific requests can be submitted through the UCSF-MAC Resource (Request form: http://memory.ucsf.edu/resources/data). Following a UCSF-regulated procedure, access will be granted to designated individuals in line with ethical guidelines on the reuse of sensitive data. This would require submission of a Material Transfer Agreement, available at: https://icd.ucsf.edu/material-transfer-and-data-agreements.

ORCID

Maria Luisa Mandelli https://orcid.org/0000-0002-2518-2520

REFERENCES

Ahmed, Z., Cooper, J., Murray, T. K., Garn, K., McNaughton, E., Clarke, H., Parhizkar, S., Ward, M. A., Cavallini, A., Jackson, S., Bose, S., Clavaguera, F., Tolnay, M., Lavenir, I., Goedert, M., Hutton, M. L., & O'Neill, M. J. (2014). A novel in vivo model of tau propagation with rapid and progressive neurofibrillary tangle pathology: The pattern of spread is determined by connectivity, not proximity. *Acta Neuropathologica*, *127*(5), 667–683. https://doi.org/10.1007/s00401-014-1254-6

Ashburner, J., & Friston, K. J. (2005). Unified segmentation. *NeuroImage*, *26*(3), 839–851. https://doi.org/10.1016/j.neuroimage.2005.02.018

Ashburner, J., & Friston, K. J. (2011). Diffeomorphic registration using geodesic shooting and Gauss-Newton optimisation. *NeuroImage*, *55*(3–3), 954–967. https://doi.org/10.1016/j.neuroimage.2010.12.049

Ashburner, J., & Ridgway, G. R. (2012). Symmetric diffeomorphic modeling of longitudinal structural MRI. *Frontiers in Neuroscience*, *6*, 197. https://doi.org/10.3389/fnins.2012.00197

Baldo, J. V., Katseff, S., & Dronkers, N. F. (2012). Brain regions underlying repetition and auditory-verbal short-term memory deficits in aphasia: Evidence from voxel-based lesion symptom mapping. *Aphasiology*, *26*(3–4), 338–354. https://doi.org/10.1080/02687038.2011.602391

Battistella, G., Borghesani, V., Henry, M., Shwe, W., Lauricella, M., Miller, Z., Deleon, J., Miller, B. L., Dronkers, N., Brambati, S. M., Seeley, W. W., Mandelli, M. L., & Gorno-Tempini, M. L. (2020). Task-free functional language networks: Reproducibility and clinical application. *The Journal of Neuroscience*, *40*(6), 1311–1320. https://doi.org/10.1523/JNEUROSCI.1485-19.2019

Brambati, S. M., Rankin, K. P., Narvid, J., Seeley, W. W., Dean, D., Rosen, H. J., Miller, B. L., Ashburner, J., & Gorno-Tempini, M. L. (2009). Atrophy progression in semantic dementia with asymmetric temporal involvement: A tensor-based morphometry study. *Neurobiology of Aging*, *30*(1), 103–111.

Brown, J. A., Deng, J., Neuhaus, J., Sible, I. J., Sias, A. C., Lee, S. E., Kornak, J., Marx, G. A., Karydas, A. M., Spina, S., Grinberg, L. T., Coppola, G., Geschwind, D. H., Kramer, J. H., Gorno-Tempini, M. L., Miller, B. L., Rosen, H. J., & Seeley, W. W. (2019). Patient-tailored, connectivity-based forecasts of spreading brain atrophy. *Neuron*, *104*(5), 856–868.e5. https://doi.org/10.1016/j.neuron.2019.08.037

Buchsbaum, B. R., & D'Esposito, M. (2009). Repetition suppression and reactivation in auditory-verbal short-term recognition memory. *Cerebral Cortex*, *19*(6), 1474–1485. https://doi.org/10.1093/cercor/bhn186

Buckner, R. L. (2004). Memory and executive function in aging and AD: Multiple factors that cause decline and reserve factors that compensate. *Neuron*, *44*(1), 195–208.

Buckner, R. L., Sepulcre, J., Talukdar, T., Krienen, F. M., Liu, H., Hedden, T., Andrews-Hanna, J. R., Sperling, R. A., & Johnson, K. A. (2009). Cortical hubs revealed by intrinsic functional connectivity: Mapping, assessment of stability, and relation to Alzheimer's disease. *Journal of Neuroscience*, *29*(6), 1860–1873. https://doi.org/10.1523/JNEUROSCI.5062-08.2009

Caspers, S., Eickhoff, S. B., Geyer, S., Scheperjans, F., Mohlberg, H., Zilles, K., & Amunts, K. (2008). The human inferior parietal lobule in stereotaxic space. *Brain Structure and Function*, *212*(6), 481–495. https://doi.org/10.1007/s00429-008-0195-z

Caspers, S., Geyer, S., Schleicher, A., Mohlberg, H., Amunts, K., & Zilles, K. (2006). The human inferior parietal cortex: Cytoarchitectonic parcellation and interindividual variability. *NeuroImage*, *33*(2), 430–448. https://doi.org/10.1016/j.neuroimage.2006.06.054

Chow, M. L., Brambati, S. M., Gorno-Tempini, M. L., Miller, B. L., & Johnson, J. K. (2010). Sound naming in neurodegenerative disease. *Brain and Cognition*, *72*(3), 423–429. https://doi.org/10.1016/j.bandc.2009.12.003

Clavaguera, F., Bolmont, T., Crowther, R. A., Abramowski, D., Frank, S., Probst, A., Fraser, G., Stalder, A. K., Beibel, M., Staufenbiel, M., Jucker, M., Goedert, M., & Tolnay, M. (2009). Transmission and spreading of tauopathy in transgenic mouse brain. *Nature Cell Biology*, *11*(7), 909–913. https://doi.org/10.1038/ncb1901

Collins, J. A., Montal, V., Hochberg, D., Quimby, M., Mandelli, M. L., Makris, N., Seeley, W. W., Gorno-Tempini, M. L., & Dickerson, B. C. (2017). Focal temporal pole atrophy and network degeneration in semantic variant primary progressive aphasia. *Brain*, *140*(2), 457–471. https://doi.org/10.1093/brain/aww313

Conca, F., Esposito, V., Giusto, G., Cappa, S. F., & Catricalà, E. (2022). Characterization of the logopenic variant of primary progressive aphasia: A systematic review and meta-analysis. *Ageing Research Reviews*, *82*-(December), 101760. https://doi.org/10.1016/j.arr.2022.101760

Cope, T. E., Rittman, T., Borchert, R. J., Simon Jones, P., Vatansever, D., Allinson, K., Passamonti, L., Vazquez Rodriguez, P., Bevan-Jones, W. R., O Brien, J. T., & Rowe, J. T. (2018). Tau burden and the functional connectome in Alzheimer's disease and progressive supranuclear palsy. *Brain*, *141*(2), 550–567. https://doi.org/10.1093/brain/awx347

Cousins, K. A. Q., Bove, J., Giannini, L. A. A., Kinney, N. G., Balgenorth, Y. R., Rascovsky, K., Lee, E. B., Trojanowski, J. Q., Grossman, M., & Irwin, D. J. (2021). Longitudinal naming and repetition relates to AD pathology and burden in autopsy-confirmed primary progressive aphasia. *Alzheimer's & Dementia*, *7*(1), e12188. https://doi.org/10.1002/trc2.12188

Cousins, K. A. Q., York, C., Bauer, L., & Grossman, M. (2016). Cognitive and anatomic double dissociation in the representation of concrete and abstract words in semantic variant and behavioral variant frontotemporal degeneration. *Neuropsychologia*, *84*(April), 244–251. https://doi.org/10.1016/j.neuropsychologia.2016.02.025

Dahnke, R., Yotter, R. A., & Gaser, C. (2013). Cortical thickness and central surface estimation. *NeuroImage*, *65*(January), 336–348. https://doi.org/10.1016/j.neuroimage.2012.09.050

Davies, R. R., Hodges, J. R., Kril, J. J., Patterson, K., Halliday, G. M., & Xuereb, J. H. (2005). The pathological basis of semantic dementia. *Brain*, *128*(Pt 9), 1984–1995. https://doi.org/10.1093/brain/awh582

de Calignon, A., Polydoro, M., Suarez-Calvet, M., William, C., Adamowicz, D. H., Kopeikina, K. J., Pitstick, R., Sahara, N., Ashe, K. H., Carlson, G. A., Spires-Jones, T. L., & Hyman, B. T (2012). Propagation of tau pathology in a model of early Alzheimer's disease. *Neuron*, *73*(4), 685–697. https://doi.org/10.1016/j.neuron.2011.11.033

DeLeon, J., Gottesman, R. F., Kleinman, J. T., Newhart, M., Davis, C., Heidler-Gary, J., Lee, A., & Hillis, A. E. (2007). Neural regions essential for distinct cognitive processes underlying picture naming. *Brain*, *130*(Pt 5), 1408–1422.

Diaz-de-Grenu, L. Z., Acosta-Cabronero, J., Chong, Y. F. V., Pereira, J. M. S., Sajjadi, S. A., Williams, G. B., & Nestor, P. J. (2014). A brief history of voxel-based grey matter analysis in Alzheimer's disease. *Journal of Alzheimer's Disease*, *38*(3), 647–659. https://doi.org/10.3233/JAD-130362

Ficek, B. N., Wang, Z., Zhao, Y., Webster, K. T., Desmond, J. E., Hillis, A. E., Frangakis, C., Faria, A. V., Caffo, B., & Tsapkini, K. (2018). The effect of TDCS on functional connectivity in primary progressive aphasia. *NeuroImage: Clinical*, *19*(May), 703–715. https://doi.org/10.1016/j.nicl.2018.05.023

Forkel, S. J., Rogalski, E., Sancho, N. D., D'Anna, L., Laguna, P. L., Sridhar, J., Dell'Acqua, F., Weintraub, S., Thompson, C., Mesulam, M. M., & Catani, M. (2020). Anatomical evidence of an indirect pathway for word repetition. *Neurology*, *94*(6), e594–e606. https://doi.org/10.1212/WNL.0000000000008746

Franzmeier, N., & Dyrba, M. (2017). Functional brain network architecture may route progression of Alzheimer's disease pathology. *Brain*, *140*(12), 3077–3080. https://doi.org/10.1093/brain/awx304

Fridriksson, J., Kjartansson, O., Morgan, P. S., Hjaltason, H., Magnusdottir, S., Bonilha, L., & Rorden, C. (2010). Impaired speech repetition and left parietal lobe damage. *The Journal of Neuroscience*, *30*(33), 11057–11061. https://doi.org/10.1523/JNEUROSCI.1120-10.2010

García, A. M., Welch, A. E., Mandelli, M. L., Henry, M. L., Lukic, S., Torres-Prioris, M. J., Deleon, J., Ratnasiri, B. M., Lorca-Puls, D. L., Miller, B. L., Seeley, W. W., Vogel, A. P., & Gorno-Tempini, M. L. (2022). Automated detection of speech timing alterations in autopsy-confirmed non-fluent/agrammatic variant primary progressive aphasia. *Neurology*, *99*(5), 500–511.

Gervits, F., Sharon Ash, H., Coslett, B., Rascovsky, K., Grossman, M., & Hamilton, R. (2016). Transcranial direct current stimulation for the treatment of primary progressive aphasia: An open-label pilot study. *Brain and Language*, *162*(November), 35–41. https://doi.org/10.1016/j.bandl.2016.05.007

Giannini, L. A. A., Irwin, D. J., McMillan, C. T., Ash, S., Rascovsky, K., Wolk, D. A., Van Deerlin, V. M., Lee, E. B., Trojanowski, J. Q., & Grossman, M. (2017). Clinical marker for Alzheimer disease pathology in logopenic primary progressive aphasia. *Neurology*, *88*(24), 2276–2284. https://doi.org/10.1212/WNL.0000000000004034

Glasser, M. F., Coalson, T. S., Robinson, E. C., Hacker, C. D., Harwell, J., Yacoub, E., Ugurbil, K., Andersson, J., Beckmann, C. F., Jenkinson, M., Smith, S. M., & van Essen, D. C. (2016). A multi-modal parcellation of human cerebral cortex. *Nature*, *536*(7615), 171–178. https://doi.org/10.1038/nature18933

Gleichgerrcht, E., Fridriksson, J., & Bonilha, L. (2015). Neuroanatomical foundations of naming impairments across different neurologic conditions. *Neurology*, *85*(3), 284–292. https://doi.org/10.1212/WNL.0000000000001765

Goedert, M., Eisenberg, D. S., & Anthony Crowther, R. (2017). Propagation of tau aggregates and neurodegeneration. *Annual Review of Neuroscience*, *40*(July), 189–210. https://doi.org/10.1146/annurev-neuro-072116-031153

Gorno-Tempini, M. L., Brambati, S. M., Ginex, V., Ogar, J., Dronkers, N. F., Marcone, A., Perani, D., Garibotto, V., Cappa, S. F., & Miller, B. L. (2008). The logopenic/phonological variant of primary progressive aphasia. *Neurology*, *71*(16), 1227–1234.

Gorno-Tempini, M. L., Dronkers, N. F., Rankin, K. P., Ogar, J. M., Phengrasamy, L., Rosen, H. J., Johnson, J. K., Weiner, M. W., &

Miller, B. L. (2004). Cognition and anatomy in three variants of primary progressive aphasia. *Annals of Neurology*, *55*(3), 335–346.

Gorno-Tempini, M. L., Hillis, A. E., Weintraub, S., Kertesz, A., Mendez, M., Cappa, S. F., Ogar, J. M., Rohrer, J. D., Black, S., Boeve, B. F., Manes, F., Dronkers, N. F., Vandenberghe, R., Rascovsky, K., Patterson, K., Miller, B. L., Knopman, D. S., Hodges, J. R., Mesulam, M. M., & Grossman, M. (2011). Classification of primary progressive aphasia and its variants. *Neurology*, *76*(11), 1006–1014.

Greicius, M. D., Srivastava, G., Reiss, A. L., & Menon, V. (2004). Default-mode network activity distinguishes Alzheimer's disease from healthy aging: Evidence from functional MRI. *Proceedings of the National Academy of Sciences of the United States of America*, *101*(13), 4637–4642.

Grossman, M. (2010). Primary progressive aphasia: Clinicopathological correlations. *Nature Reviews. Neurology*, *6*(2), 88–97. https://doi.org/10.1038/nrneurol.2009.216

Harris, J. M., & Jones, M. (2014). Pathology in primary progressive aphasia syndromes. *Current Neurology and Neuroscience Reports*, *14*(8), 466. https://doi.org/10.1007/s11910-014-0466-4

Henry, M. L., & Gorno-Tempini, M. L. (2010). The logopenic variant of primary progressive aphasia. *Current Opinion in Neurology*, *23*(6), 633–637. https://doi.org/10.1097/WCO.0b013e32833fb93e

Hickok, G., & Poeppel, D. (2004). Dorsal and ventral streams: A framework for understanding aspects of the functional anatomy of language. *Cognition*, *92*(1–2), 67–99. https://doi.org/10.1016/j.cognition.2003.10.011

Hogstrom, L. J., Westlye, L. T., Walhovd, K. B., & Fjell, A. M. (2013). The structure of the cerebral cortex across adult life: Age-related patterns of surface area, thickness, and gyrification. *Cerebral Cortex*, *23*(11), 2521–2530. https://doi.org/10.1093/cercor/bhs231

Hu, W. T., McMillan, C., Libon, D., Leight, S., Forman, M., Lee, V. M.-Y., Trojanowski, J. Q., & Grossman, M. (2010). Multimodal predictors for Alzheimer disease in nonfluent primary progressive aphasia. *Neurology*, *75*(7), 595–602. https://doi.org/10.1212/WNL.0b013e3181ed9c52

Iba, M., Guo, J. L., McBride, J. D., Zhang, B., Trojanowski, J. Q., & Lee, V. M.-Y. (2013). Synthetic tau fibrils mediate transmission of neurofibrillary tangles in a transgenic mouse model of Alzheimer's-like tauopathy. *Journal of Neuroscience*, *33*(3), 1024–1037. https://doi.org/10.1523/JNEUROSCI.2642-12.2013

Indefrey, P., & Levelt, W. J. M. (2004). The spatial and temporal signatures of word production components. *Cognition*, *92*(1–2), 101–144. https://doi.org/10.1016/j.cognition.2002.06.001

Joie, L., Renaud, N. A., Seeley, W. W., Borys, E., Boxer, A. L., DeCarli, C., Doré, V., Grinberg, L. T., Huang, E., Hwang, J. H., Ikonomovic, M. D., Jack, C. Jr., Jagust, W. J., Jin, L. W., Klunk, W. E., Kofler, J., Lesman-Segev, O. H., Lockhart, S. N., Lowe, V. J., ..., Rabinovici, G. D. (2019). Multisite study of the relationships between antemortem [11C]PIB-PET centiloid values and postmortem measures of Alzheimer's disease neuropathology. *Alzheimer's & Dementia*, *15*(2), 205–216. https://doi.org/10.1016/j.jalz.2018.09.001

Josephs, K. A., Duffy, J. R., Strand, E. A., Whitwell, J. L., Layton, K. F., Parisi, J. E., Hauser, M. F., Witte, R. J., Boeve, B. F., Knopman, D. S., Dickson, D. W., Jack, C. R., Jr., & Petersen, R. C. (2006). Clinicopathological and imaging correlates of progressive aphasia and apraxia of speech. *Brain*, *129*(Pt 6), 1385–1398. https://doi.org/10.1093/brain/awl078

Joubert, S., Vallet, G. T., Montembeault, M., Boukadi, M., Wilson, M. A., Laforce, R. J., Rouleau, I., & Brambati, S. M. (2017). Comprehension of concrete and abstract words in semantic variant primary progressive aphasia and Alzheimer's disease: A behavioral and neuroimaging study. *Brain and Language*, *170*(July), 93–102. https://doi.org/10.1016/j.bandl.2017.04.004

Kaplan, E. F., Goodglass, H., & Weintraub, S. (1983). *The Boston naming test*. Lea & Febiger.

Kertesz, A. (1980). *Western aphasia battery*. University of Western Ontario Press.

Kertesz, A., McMonagle, P., Blair, M., Davidson, W., & Munoz, D. G. (2005). The evolution and pathology of frontotemporal dementia. *Brain*, *128*(Pt 9), 1996–2005. https://doi.org/10.1093/brain/awh598

Kirshner, H. S. (2012). Primary progressive aphasia and Alzheimer's disease: Brief history, recent evidence. *Current Neurology and Neuroscience Reports*, *12*(6), 709–714. https://doi.org/10.1007/s11910-012-0307-2

Kramer, J. H., Jurik, J., Sha, S. J., Rankin, K. P., Rosen, H. J., Johnson, J. K., & Miller, B. L. (2003). Distinctive neuropsychological patterns in frontotemporal dementia, semantic dementia, and Alzheimer disease. *Cognitive and Behavioral Neurology*, *16*(4), 211–218.

Lehmann, M., Ghosh, P. M., Madison, C., Laforce, R., Jr., Corbetta-Rastelli, C., Weiner, M. W., Greicius, M. D., Seeley, W. W., Gorno-Tempini, M. L., Rosen, H. J., Miller, B. L., Jagust, W. J., & Rabinovici, G. D. (2013). Diverging patterns of amyloid deposition and hypometabolism in clinical variants of probable Alzheimer's disease. *Brain*, *136*(Pt 3), 844–858. https://doi.org/10.1093/brain/aws327

Lehmann, M., Madison, C. M., Ghosh, P. M., Seeley, W. W., Mormino, E., Greicius, M. D., Gorno-Tempini, M. L., Kramer, J. H., Miller, B. L., Jagust, W. J., & Rabinovici, G. D. (2013). Intrinsic connectivity networks in healthy subjects explain clinical variability in Alzheimer's disease. *Proceedings of the National Academy of Sciences of the United States of America*, *110*(28), 11606–11611. https://doi.org/10.1073/pnas.1221536110

Lesman-Segev, O., La Joie, R., Iaccarino, L., Lobach, I., Rosen, H., Seo, S. W., Janabi, M., Baker, S. L., Edwards, L., Pham, J., Olichney, J., Boxer, A., Huang, E., Gorno-Tempini, M., DeCarli, C., Hepker, M., Hwang, J. H. L., Miller, B. L., Spina, S., ... Rabinovici, G. D. (2020). Diagnostic accuracy of amyloid versus FDG PET in autopsy-confirmed dementia. *Annals of Neurology*, *89*(2), 389–401. https://doi.org/10.1002/ana.25968.

Leyton, C. E., Hodges, J. R., McLean, C. A., Kril, J. J., Piguet, O., & Ballard, K. J. (2015). Is the logopenic-variant of primary progressive aphasia a unitary disorder? *Cortex*, *67*, 122–133. https://doi.org/10.1016/j.cortex.2015.03.011

Liu, L., Drouet, V., Wu, J. W., Witter, M. P., Small, S. A., Clelland, C., & Duff, K. (2012). Trans-synaptic spread of tau pathology in vivo. *PLoS One*, *7*(2), e31302. https://doi.org/10.1371/journal.pone.0031302

Louwersheimer, E., Antoinette Keulen, M., Steenwijk, M. D., Wattjes, M. P., Jiskoot, L. C., Vrenken, H., Teunissen, C. E., van Berckel, B. N., van der Flier, W. M., Scheltens, P., van Swieten, J. C., & Pijnenburg, Y. A. (2016). Heterogeneous language profiles in patients with primary progressive aphasia due to Alzheimer's disease. *Journal of Alzheimer's Disease*, *51*(2), 581–590. https://doi.org/10.3233/JAD-150812

Lukic, S., Mandelli, M. L., Welch, A., Jordan, K., Shwe, W., Neuhaus, J., Miller, Z., Hubbard, H. I., Henry, M., Miller, B. L., Dronkers, N. F., & Gorno-Tempini, M. L. (2019). Neurocognitive basis of repetition deficits in primary progressive aphasia. *Brain and Language*, *194*(July), 35–45. https://doi.org/10.1016/j.bandl.2019.04.003

Machulda, M. M., Whitwell, J. L., Duffy, J. R., Strand, E. A., Dean, P. M., Senjem, M. L., Jack, C. R., Jr., & Josephs, K. A. (2013). Identification of an atypical variant of logopenic progressive aphasia. *Brain and Language*, *127*(2), 139–144. https://doi.org/10.1016/j.bandl.2013.02.007

Majerus, S. (2013). Language repetition and short-term memory: An integrative framework. *Frontiers in Human Neuroscience*, *7*, 357. https://doi.org/10.3389/fnhum.2013.00357

Mandelli, M. L., Caverzasi, E., Binney, R. J., Henry, M. L., Lobach, I., Block, N., Amirbekian, B., Dronkers, N., Miller, B. L., Henry, R. G., & Gorno-Tempini, M. L. (2014). Frontal white matter tracts sustaining speech production in primary progressive aphasia. *The Journal of Neuroscience*, *34*(29), 9754–9767. https://doi.org/10.1523/JNEUROSCI.3464-13.2014

Mandelli, M. L., Vilaplana, E., Brown, J. A., Isabel Hubbard, H., Binney, R. J., Attygalle, S., Santos-Santos, M. A., Miller, Z. A., Pakvasa, M., Henry,

M. L., Rosen, H. G., Henry, R. G., Rabinovici, G. D., Miller, B. L., Seeley, W. W., & Gorno-Tempini, M. L. (2016). Healthy brain connectivity predicts atrophy progression in non-fluent variant of primary progressive aphasia. *Brain*, *139*(Pt 10), 2778–2791. https://doi.org/10.1093/brain/aww195

Mandelli, M. L., Welch, A. E., Vilaplana, E., Watson, C., Battistella, G., Brown, J. A., Possin, K. L., Hubbard, H. I., Miller, Z. A., Henry, M. L., Marx, G. A., Santos-Santos, M. A., Bajorek, L. P., Fortea, J., Boxer, A., Rabinovici, G., Lee, S., Deleon, J., Rosen, H. J., … Gorno-Tempini, M. L. (2018). Altered topology of the functional speech production network in non-fluent/agrammatic variant of PPA. *Cortex*, *108*, 252–264. https://doi.org/10.1016/j.cortex.2018.08.002

Manjón, J. V., Coupé, P., Luis Martí-Bonmatí, D., Collins, L., & Robles, M. (2010). Adaptive non-local means denoising of MR images with spatially varying noise levels. *Journal of Magnetic Resonance Imaging*, *31*(1), 192–203. https://doi.org/10.1002/jmri.22003

Mesulam, M. (2008). Primary progressive aphasia pathology. *Annals of Neurology*, *63*(1), 124–125. https://doi.org/10.1002/ana.20940

Mesulam, M., Weineke, C., Rogalski, E., Cobia, D., Thompson, C., & Weintraub, S. (2009). Quantitative template for subtyping primary progressive aphasia. *Archives of Neurology*, *66*(12), 1545–1551.

Mesulam, M.-M., Rogalski, E. J., Wieneke, C., Hurley, R. S., Geula, C., Bigio, E. H., Thompson, C. K., & Weintraub, S. (2014). Primary progressive aphasia and the evolving neurology of the language network. *Nature Reviews. Neurology*, *10*(10), 554–569. https://doi.org/10.1038/nrneurol.2014.159

Mesulam, M., Wicklund, A., Johnson, N., Rogalski, E., Léger, G. C., Rademaker, A., Weintraub, S., & Bigio, E. H. (2008). Alzheimer and frontotemporal pathology in subsets of primary progressive aphasia. *Annals of Neurology*, *63*(6), 709–719. https://doi.org/10.1002/ana.21388

Migliaccio, R., Agosta, F., Rascovsky, K., Karydas, A., Bonasera, S., Rabinovici, G. D., Miller, B. L., & Gorno-Tempini, M. L. (2009). Clinical syndromes associated with posterior atrophy: Early age at onset AD spectrum. *Neurology*, *73*(19), 1571–1578.

Migliaccio, R., Boutet, C., Valabregue, R., Ferrieux, S., Nogues, M., Lehéricy, S., Dormont, D., Levy, R., Dubois, B., & Teichmann, M. (2016). The brain network of naming: A lesson from primary progressive aphasia. *PLoS One*, *11*(2), e0148707. https://doi.org/10.1371/journal.pone.0148707

Miller, H. E., Cordella, C., Collins, J. A., Ezzo, R., Quimby, M., Hochberg, D., Tourville, J. A., Dickerson, B. C., & Guenther, F. H. (2021). Neural substrates of verbal repetition deficits in primary progressive aphasia. *Brain Communications*, *3*(1), fcab015. https://doi.org/10.1093/braincomms/fcab015

Milton, C. K., Dhanaraj, V., Young, I. M., Taylor, H. M., Nicholas, P. J., Briggs, R. G., Bai, M. Y., Fonseka, R. D., Hormovas, J., Lin, Y. H., Tanglay, O., Conner, A. K., Glenn, C. A., Teo, C., Doyen, S., & Sughrue, M. E. (2021). Parcellation-based anatomic model of the semantic network. *Brain and Behavior*, *11*(4), e02065. https://doi.org/10.1002/brb3.2065

Nissim, N. R., Moberg, P. J., & Hamilton, R. H. (2020). Efficacy of noninvasive brain stimulation (TDCS or TMS) paired with language therapy in the treatment of primary progressive aphasia: An exploratory meta-analysis. *Brain Sciences*, *10*(9), 597. https://doi.org/10.3390/brainsci10090597

Ossenkoppele, R., Cohn-Sheehy, B. I., La Joie, R., Vogel, J. W., Moller, C., Lehmann, M., van Berckel, B. N., Seeley, W. W., Pijnenburg, Y. A., Gorno-Tempini, M. L., Kramer, J. H., Barkhof, F., Rosen, H. J., van der Flier, W. M., Jagust, W. J., Miller, B. L., Scheltens, P., & Rabinovici, G. D. (2015). Atrophy patterns in early clinical stages across distinct phenotypes of Alzheimer's disease. *Human Brain Mapping*, *36*, 4421–4437. https://doi.org/10.1002/hbm.22927

Ossenkoppele, R., Schonhaut, D. R., Schöll, M., Lockhart, S. N., Ayakta, N., Baker, S. L., O'Neil, J. P., Janabi, M., Lazaris, M., Cantwell, A., Vogel, J., Santos, M., Miller, Z. A., Bettcher, B. M., Vossel, K. A., Kramer, J. H., Gorno-Tempini, M. L., Miller, B. L., Jagust, W. J., & Rabinovici, G. D. (2016). Tau PET patterns mirror clinical and neuroanatomical variability in Alzheimer's disease. *Brain*, *139*(5), 1551–1567. https://doi.org/10.1093/brain/aww027

Phillips, J. S., Da Re, F., Dratch, L., Xie, S. X., Irwin, D. J., McMillan, C. T., Vaishnavi, S. N., Ferrarese, C., Lee, E. B., Shaw, L. M., Trojanowski, J. Q., Wolk, D. A., & Grossman, M. (2018). Neocortical origin and progression of gray matter atrophy in nonamnestic Alzheimer's disease. *Neurobiology of Aging*, *63*(March), 75–87. https://doi.org/10.1016/j.neurobiolaging.2017.11.008

Preiß, D., Billette, O. V., Schneider, A., Spotorno, N., & Nestor, P. J. (2019). The atrophy pattern in Alzheimer-related PPA is more widespread than that of the frontotemporal lobar degeneration associated variants. *NeuroImage: Clinical*, *24*(January), 101994. https://doi.org/10.1016/j.nicl.2019.101994

Pruim, R. H. R., Mennes, M., van Rooij, D., Llera, A., Buitelaar, J. K., & Beckmann, C. F. (2015). ICA-AROMA: A robust ICA-based strategy for removing motion artifacts from FMRI data. *NeuroImage*, *112*(May), 267–277. https://doi.org/10.1016/j.neuroimage.2015.02.064

Prusiner, S. B. (1984). Prions. *Scientific American*, *251*(4), 50–59. https://doi.org/10.1038/scientificamerican1084-50

Rabinovici, G. D., Jagust, W. J., Furst, A. J., Ogar, J. M., Racine, C. A., Mormino, E. C., O'Neil, J. P., Lal, R. A., Dronkers, N. F., Miller, B. L., & Gorno-Tempini, M. L. (2008). Abeta amyloid and glucose metabolism in three variants of primary progressive aphasia. *Annals of Neurology*, *64*(4), 388–401. https://doi.org/10.1002/ana.21451

Rajapakse, J. C., Giedd, J. N., & Rapoport, J. L. (1997). Statistical approach to segmentation of single-channel cerebral MR images. *IEEE Transactions on Medical Imaging*, *16*(2), 176–186. https://doi.org/10.1109/42.563663

Ramanan, S., Irish, M., Patterson, K., Rowe, J. B., Gorno-Tempini, M. L., & Lambon Ralph, M. A. (2022). Understanding the multidimensional cognitive deficits of logopenic variant primary progressive aphasia. *Brain*, *145*(9), 2955–2966. https://doi.org/10.1093/brain/awac208

Reuter, M., & Fischl, B. (2011). Avoiding asymmetry-induced bias in longitudinal image processing. *NeuroImage*, *57*(1), 19–21. https://doi.org/10.1016/j.neuroimage.2011.02.076

Reuter, M., Schmansky, N. J., Diana Rosas, H., & Fischl, B. (2012). Within-subject template estimation for unbiased longitudinal image analysis. *NeuroImage*, *61*(4), 1402–1418. https://doi.org/10.1016/j.neuroimage.2012.02.084

Rogalski, E., Cobia, D., Harrison, T. M., Wieneke, C., Weintraub, S., & Mesulam, M. M. (2011). Progression of language decline and cortical atrophy in subtypes of primary progressive aphasia. *Neurology*, *76*(21), 1804–1810. https://doi.org/10.1212/WNL.0b013e31821ccd3c

Rogalski, E., Cobia, D., Harrison, T. M., Wieneke, C., Thompson, C. K., Weintraub, S., & Mesulam, M. M. (2011). Anatomy of language impairments in primary progressive aphasia. *The Journal of Neuroscience*, *31*(9), 3344–3350. https://doi.org/10.1523/JNEUROSCI.5544-10.2011

Rogalski, E., Sridhar, J., Rader, B., Martersteck, A., Chen, K., Cobia, D., Thompson, C. K., Weintraub, S., Bigio, E. H., & Mesulam, M. M. (2016). Aphasic variant of Alzheimer disease: Clinical, anatomic, and genetic features. *Neurology*, *87*(13), 1337–1343. https://doi.org/10.1212/WNL.0000000000003165

Rogalsky, C., Poppa, T., Chen, K.-H., Anderson, S. W., Damasio, H., Love, T., & Hickok, G. (2015). Speech repetition as a window on the neurobiology of auditory-motor integration for speech: A voxel-based lesion symptom mapping study. *Neuropsychologia*, *71*(May), 18–27. https://doi.org/10.1016/j.neuropsychologia.2015.03.012

Rohrer, J. D., Caso, F., Mahoney, C., Henry, M., Rosen, H. J., Rabinovici, G., Rossor, M. N., Miller, B., Warren, J. D., Fox, N. C., Ridgway, G. R., & Gorno-Tempini, M. L. (2013). Patterns of longitudinal brain atrophy in the logopenic variant of primary progressive aphasia. *Brain and Language*, *127*, 121–126. https://doi.org/10.1016/j.bandl.2012.12.008

Rohrer, J. D., Rossor, M. N., & Warren, J. D. (2012). Alzheimer's pathology in primary progressive aphasia. *Neurobiology of Aging*, *33*(4), 744–752. https://doi.org/10.1016/j.neurobiolaging.2010.05.020

Rosen, H. J., Gorno-Tempini, M. L., Goldman, W. P., Perry, R. J., Schuff, N., Weiner, M., Feiwell, R., Kramer, J. H., & Miller, B. L. (2002). Patterns of brain atrophy in frontotemporal dementia and semantic dementia. *Neurology*, *58*(2), 198–208.

Rubinov, M., & Sporns, O. (2010). Complex network measures of brain connectivity: Uses and interpretations. *NeuroImage*, *52*(3), 1059–1069. https://doi.org/10.1016/j.neuroimage.2009.10.003

Sajjadi, S. A., Patterson, K., Arnold, R. J., Watson, P. C., & Nestor, P. J. (2012). Primary progressive aphasia. *Neurology*, *78*(21), 1670–1677. https://doi.org/10.1212/WNL.0b013e3182574f79

Seeley, W. W., Crawford, R. K., Zhou, J., Miller, B. L., & Greicius, M. D. (2009). Neurodegenerative diseases target large-scale human brain networks. *Neuron*, *62*(1), 42–52.

Seeley, W. W., Menon, V., Schatzberg, A. F., Keller, J., Glover, G. H., Kenna, H., Reiss, A. L., & Greicius, M. D. (2007). Dissociable intrinsic connectivity networks for salience processing and executive control. *Journal of Neuroscience*, *27*(9), 2349–2356. https://doi.org/10.1523/JNEUROSCI.5587-06.2007

Snowden, J., Neary, D., & Mann, D. (2007). Frontotemporal lobar degeneration: Clinical and pathological relationships. *Acta Neuropathologica*, *114*(1), 31–38. https://doi.org/10.1007/s00401-007-0236-3

Spinelli, E. G., Mandelli, M. L., Miller, Z. A., Santos-Santos, M. A., Wilson, S. M., Agosta, F., Grinberg, L. T., Huang, E. J., Trojanowski, J. Q., Meyer, M., Henry, M. L., Comi, G., Rabinovici, G., Rosen, H. J., Filippi, M., Miller, B. L., Seeley, W. W., & Gorno-Tempini, M. L. (2017). Typical and atypical pathology in primary progressive aphasia variants. *Annals of Neurology*, *81*(3), 430–443. https://doi.org/10.1002/ana.24885

Teichmann, M., Kas, A., Boutet, C., Ferrieux, S., Nogues, M., Samri, D., Rogan, C., Dormont, D., Dubois, B., & Migliaccio, R. (2013). Deciphering logopenic primary progressive aphasia: A clinical, imaging and biomarker investigation. *Brain*, *136*(Pt 11), 3474–3488. https://doi.org/10.1093/brain/awt266

Tohka, J., Zijdenbos, A., & Evans, A. (2004). Fast and robust parameter estimation for statistical partial volume models in brain MRI. *NeuroImage*, *23*(1), 84–97. https://doi.org/10.1016/j.neuroimage.2004.05.007

Tsapkini, K., Webster, K. T., Ficek, B. N., Desmond, J. E., Onyike, C. U., Rapp, B., Frangakis, C. E., & Hillis, A. E. (2018). Electrical brain stimulation in different variants of primary progressive aphasia: A randomized clinical trial. *Alzheimer's & Dementia*, *4*, 461–472. https://doi.org/10.1016/j.trci.2018.08.002

Villeneuve, S., Rabinovici, G. D., Cohn-Sheehy, B. I., Madison, C., Ayakta, N., Ghosh, P. M., La Joie, R., Arthur-Bentil, S. K., Vogel, J. W., Marks, S. M., Lehmann, M., Rosen, H. J., Reed, B., Olichney, J., Boxer, A. L., Miller, B. L., Borys, E., Jin, L. W., Huang, E. J., … Jagust, W. (2015). Existing Pittsburgh compound-B positron emission tomography thresholds are too high: Statistical and pathological evaluation. *Brain*, *138*(Pt 7), 2020–2033. https://doi.org/10.1093/brain/awv112

Vogel, J. W., Iturria-Medina, Y., Strandberg, O. T., Smith, R., Levitis, E., Evans, A. C., & Hansson, O. (2020). Spread of pathological tau proteins through communicating neurons in human Alzheimer's disease. *Nature Communications*, *11*(1), 2612. https://doi.org/10.1038/s41467-020-15701-2

Watson, C. L., Possin, K., Allen, I. E., Hubbard, H. I., Meyer, M., Welch, A. E., Rabinovici, G. D., Rosen, H., Rankin, K. P., Miller, Z., Santos-Santos, M. A., Kramer, J. H., Miller, B. L., & Gorno-Tempini, M. L. (2018). Visuospatial functioning in the primary progressive aphasias. *Journal of the International Neuropsychological Society*, *24*(3), 259–268. https://doi.org/10.1017/S1355617717000984

Whitwell, J. L., Martin, P., Graff-Radford, J., Machulda, M. M., Senjem, M. L., Schwarz, C. G., Weigand, S. D., Spychalla, A. J., Drubach, D. A., Jack, C. R., Jr., Lowe, V. J., & Josephs, K. A. (2019). The role of age on tau PET uptake and grey matter atrophy in atypical Alzheimer disease. *Alzheimer's & Dementia*, *15*(5), 675–685. https://doi.org/10.1016/j.jalz.2018.12.016

Wilson, S. M., Dronkers, N. F., Ogar, J. M., Jang, J., Growdon, M. E., Agosta, F., Henry, M. L., Miller, B. L., & Gorno-Tempini, M. L. (2010). Neural correlates of syntactic processing in the nonfluent variant of primary progressive aphasia. *Journal of Neuroscience*, *30*(50), 16845–16854. https://doi.org/10.1523/JNEUROSCI.2547-10.2010

Wilson, S. M., Henry, M. L., Besbris, M., Ogar, J. M., Dronkers, N. F., Jarrold, W., Miller, B. L., & Gorno-Tempini, M. L. (2010). Connected speech production in three variants of primary progressive aphasia. *Brain*, *133*(Pt 7), 2069–2088.

Yotter, R. A., Nenadic, I., Ziegler, G., Thompson, P. M., & Gaser, C. (2011). Local cortical surface complexity maps from spherical harmonic reconstructions. *NeuroImage*, *56*(3), 961–973. https://doi.org/10.1016/j.neuroimage.2011.02.007

Yotter, R. A., Dahnke, R., Thompson, P. M., & Gaser, C. (2010). Topological correction of brain surface meshes using spherical harmonics. *Human Brain Mapping*, *32*(7), 1109–1124. https://doi.org/10.1002/hbm.21095

Zhou, J., Gennatas, E. D., Kramer, J. H., Miller, B. L., & Seeley, W. W. (2012). Predicting regional neurodegeneration from the healthy brain functional connectome. *Neuron*, *73*(6), 1216–1227. https://doi.org/10.1016/j.neuron.2012.03.004

Zhou, J., Greicius, M. D., Gennatas, E. D., Growdon, M. E., Jang, J. Y., Rabinovici, G. D., Kramer, J. H., Weiner, M., Miller, B. L., & Seeley, W. W. (2010). Divergent network connectivity changes in behavioural variant frontotemporal dementia and Alzheimer's disease. *Brain*, *133*(Pt 5), 1352–1367.

SUPPORTING INFORMATION

Additional supporting information can be found online in the Supporting Information section at the end of this article.

How to cite this article: Mandelli, M. L., Lorca-Puls, D. L., Lukic, S., Montembeault, M., Gajardo-Vidal, A., Licata, A., Scheffler, A., Battistella, G., Grasso, S. M., Bogley, R., Ratnasiri, B. M., La Joie, R., Mundada, N. S., Europa, E., Rabinovici, G., Miller, B. L., De Leon, J., Henry, M. L., Miller, Z., & Gorno-Tempini, M. L. (2023). Network anatomy in logopenic variant of primary progressive aphasia. *Human Brain Mapping*, *44*(11), 4390–4406. https://doi.org/10.1002/hbm.26388